Bone morphogenetic protein 7 (BMP-7) increases the expression of follicle-stimulating hormone (FSH) receptor in human granulosa cells

Jia Shi, M.D.,[a] *Osamu Yoshino, M.D., Ph.D.,*[a,b] *Yutaka Osuga, M.D., Ph.D.,*[a] *Osamu Nishii, M.D., Ph.D.,*[b] *Tetsu Yano, M.D., Ph.D.,*[a] *and Yuji Taketani, M.D., Ph.D.*[a]

[a] Department of Obstetrics and Gynecology, University of Tokyo, Tokyo; and [b] Department of Obstetrics and Gynecology, Mizonokuchi Hospital, Teikyo University, Kawasaki, Japan

Objective: To examine the effect of bone morphogenetic protein 7 (BMP-7) on FSH receptor (FSHR) expression in human granulosa cells.
Design: Laboratory study using human samples.
Setting: University hospital.
Patient(s): Human granulosa cells were obtained from 60 women undergoing oocyte retrieval for IVF.
Intervention(s): Human granulosa cells (GCs) were cultured with recombinant BMP-7, followed by RNA extraction.
Main Outcome Measure(s): mRNA levels of GCs were measured by real-time reverse-transcription polymerase chain reaction.
Result(s): Bone morphogenetic protein 7 increased FSHR gene expression in human luteinized granulosa cells, whereas it decreased LH receptor gene expression. Bone morphogenetic protein 7 also increased FSH-induced cyclic adenosine monophosphate production in GCs, indicating up-regulation of the cellular response to FSH. Although BMP-7 increased gene expression of activin-βA and -βB in GCs, inhibition of activin function did not affect the BMP-7–induced FSHR gene expression.
Conclusion(s): These findings provide new insight into the biologic function of BMP-7 in the human ovary and demonstrate its unique mechanism of regulating FSHR action. (Fertil Steril® 2009; ■: ■–■. ©2009 by American Society for Reproductive Medicine.)

Key Words: BMP, FSH receptor, ovary, folliculogenesis, female fertility

The pituitary gonadotropin FSH is a key hormone in the regulation of folliculogenesis and female fertility (1, 2). In the ovary, FSH triggers cytodifferentiation and proliferation of granulosa cells (GCs), ultimately resulting in the development of preovulatory follicles (3, 4).

Because FSH acts on the ovary in an endocrine manner, the expression of FSH receptor (FSHR) on target cells is essential for modulation of ovarian function by FSH. It is well known that FSHR is not expressed until midway through follicle development. In mature follicles, maintenance of FSHR expression is required to avoid death by atresia (5–7). Therefore, it is important to elucidate the mechanism responsible for regulation of FSHR expression to better understand the process of folliculogenesis.

Several factors, such as activins (8, 9), FSH (10), cyclic adenosine monophosphate (cAMP) stimulants and cAMP analogs (11), are known to modulate the synthesis of FSHR mRNA in GCs. Recently, the bone morphogenetic proteins (BMPs), which are members of the transforming growth factor-β superfamily, have emerged as important players in ovarian physiology and female fertility (12, 13). There is growing evidence that BMP-7 can modulate steroidogenesis in a way that promotes estrogen production while inhibiting progesterone biosynthesis in many species (14–16). Bone morphogenetic protein 7 increases FSH mRNA levels in cultured mouse ovaries (18). However, no information is available on the effect of BMP-7 on human primary GCs, although Abir et al. (17) reported that BMP-7 and its receptors are expressed in human ovarian follicles. In view of the finding that BMP-7 is expressed from small follicles (17), we hypothesized that BMP-7 might increase FSHR mRNA levels in human ovarian follicles. In this study, we investigated the effect of BMP-7 on FSHR expression using cultured human luteinized granulosa cells (LGCs), aiming to elucidate possible roles of BMP-7 in the human ovary.

Received May 12, 2008; revised October 10, 2008; accepted November 11, 2008.
J.S. has nothing to disclose. O.Y. has nothing to disclose. Y.O. has nothing to disclose. O.N. has nothing to disclose. T.Y. has nothing to disclose. Y.T. has nothing to disclose.
Supported in part by Health and Labor Sciences Research Grants from the Ministry of Health, Labor, and Welfare of Japan, Grant-in-Aid for Scientific Research from the Ministry of Education, Culture, Sports, Science, and Technology, Kowa Life Science Foundation, and Kanzawa Science Foundation.
Reprint requests: Yutaka Osuga, Department of Obstetrics and Gynecology, Faculty of Medicine, University of Tokyo, 7-3-1, Hongo, Bunkyo-ku, Tokyo, 113-8655, Japan (FAX: +81-3-3816-2017; E-mail: yutakaos-tky@umin.ac.jp).

MATERIALS AND METHODS

Reagents and Materials

Hyaluronidase, fetal bovine serum (FBS), DMEM/F12, and antibiotics (mixture of penicillin, streptomycin, and amphotericin B) were purchased from Sigma (St. Louis, MO), recombinant human BMP-7 was purchased from R&D Systems (Minneapolis, MN), and SB-431542 was from Calbiochem (La Jolla,

0015-0282/09/$36.00
doi:10.1016/j.fertnstert.2008.11.014

CA). Recombinant human FSH and activin-A were kindly provided by Nippon Organon (Tokyo, Japan) and Dr. Shunichi Shimasaki (University of California, San Diego), respectively.

Cell Culture of Human Luteinized Granulosa Cells

The method to obtain and culture human LGCs was described previously (19–21). Briefly, follicular fluid with LGCs was aspirated from 60 patients undergoing ovarian stimulation for in vitro fertilization (IVF). The clinical reasons for IVF in these patients were primarily male factor or tubal factor infertility. Patients with ovarian dysfunction were excluded from the study. The experimental procedures were approved by the institutional review board, and signed informed consent for use of LGCs was obtained from each patient. All of the follicular aspirates from each patient were pooled and centrifuged at 200*g* for 5 min, resuspended in phosphate-buffered saline (PBS) with 0.2% hyaluronidase, and incubated at 37°C for 30 min. The suspension was layered onto Ficoll-Paque and centrifuged at 150*g* for 20 min. The LGCs were collected from the interphase, washed with PBS, and cultured in DMEM/F12 medium supplemented with 5% FBS and antibiotics (100 U/mL penicillin, 0.1 mg/mL streptomycin, and 250 ng/mL amphotericin B) for 15 min at 37°C to remove contaminating macrophage cells from LGCs. Using this procedure, LGCs were isolated in the supernatant and macrophages were attached to the culture dish. The collected human LGCs were cultured in DMEM/F12 containing 5% FBS and antibiotics in 12-well plates at a density of 2×10^5 cells/mL and kept at 37°C in a humidified 5% CO_2/95% air environment for 5 days. With this method, the contamination of monocyte/macrophages and endothelial cells were less than 1 % judged by immunohistochemistry for CD68 and von Willebrand factor, respectively (data not shown). All of the LGCs used for the experiments were precultured for 5 days before treatments to allow the LGCs to regain sensitivity to FSH stimulation (22). The media were changed at 48 hr intervals. To evaluate the effects of BMP-7, human LGCs were cultured with or without BMP-7 (100 ng/mL) for 24 hr. In a dose-response study, LGCs were cultured with increasing concentrations of BMP-7 (0–300 ng/mL) for 24 h. In the time course experiments, LGCs were incubated with or without BMP-7 (100 ng/mL) for 3, 8, 24, and 48 h. To investigate which BMP receptor was used for induction of FSHR by BMP-7, activin receptor–like kinase (ALK) 4, 5, and 7 inhibitor SB-431542 was used before stimulation with BMP-7 or activin-A. Recombinant BMP-7 was dissolved in 0.1% BSA + 4 mmol/L HCl, and SB-431542 was dissolved in dimethylsulfoxide as vehicle. The same amount of vehicle was used for control.

Reverse Transcription and Quantitative Real-Time Polymerase Chain Reaction Analysis

Total RNA was extracted from LGCs using the RNAeasy minikit (Qiagen, Hilden, Germany). Reverse transcription (RT) was performed using Rever Tra Dash (Toyobo, Tokyo, Japan). One microgram of total RNA was reverse transcribed in a 20-μL volume. For the quantification of various mRNA levels, real-time polymerase chain reaction (PCR) was performed using LightCycler (Roche Diagnostic, Mannheim, Germany) according to the manufacturer's instructions. The PCR primers were selected from different exons of the corresponding genes to discriminate PCR products that might arise from possible chromosomal DNA contaminants. The primer sequences were as follows, FSHR (NM_000145: 174–196 and 510–492), inhibin-α (NM_002191: 369–388 and 602–582), inhibin/activin-βA (NM_002192: 505–526 and 673–653), inhibin/activin-βB (NM_002193: 1184–1204 and 1325–1305), LH receptor (LHR) (NM_000233:747–767 and 981–962), ALK-6 (NM_001203: 356–375 and 761–742), BMPR-II (NM_001204: 647–666 and 1075–1054), and GAPDH (NM_002046: 628–648 and 1079–1060) (21). The PCR conditions for FSHR, inhibin-α, and inhibin/activin-βA and -βB consisted of 40 cycles at 95°C for 10 s, 55°C for 10 s, and 72°C for 14 s, followed by melting curve analysis. The PCR conditions for LHR consisted of 40 cycles at 95°C for 10 s, 60°C for 10 s, and 72°C for 9 s, followed by melting curve analysis. The PCR conditions for GAPDH consisted of 35 cycles at 95°C for 10 s, 64°C for 10 s, and 72°C for 18 s, followed by melting curve analysis. Expression of each mRNA was normalized by GAPDH mRNA. The temperature condition for regular PCR was 94°C for 10 s, 55°C for 4 s, and 72°C for 30 s. The number of PCR cycles was 22 for GAPDH, 25 for inhibin-α and inhibin/activin-βA, 30 for ALK-6 and BMPR-II, and 33 for inhibin/activin-βB, FSHR, and LHR. The PCR products were analyzed by 2% agarose gel electrophoresis with ethidium bromide.

Measurement of cAMP Levels

To assess the level of cAMP synthesis, LGCs were cultured in 48-well plates with DMEM/F12 containing 1% FBS and antibiotics with or without BMP-7 (100 ng/mL) for 24 h. Then cells were cultured with 0.1 mmol/L IBMX, a phosphodiesterase inhibitor, in the presence or absence of FSH (0.5 IU/mL) for 2 h. Conditioned medium was collected and the extracellular content of cAMP was determined using a cAMP enzyme immunoassay kit (Caymen Chemical Company, Ann Arbor, Michigan).

Statistical Analysis

All results are shown as mean ± SD of data from at least three separate experiments, each performed with triplicate samples. Data were analyzed by Student *t* test for paired comparison and one-way analysis of variance with post hoc test for multiple comparisons using Statview software (SAS Institute, Cary, NC). A P value of $< .05$ was considered to be statistically significant.

RESULTS

Effect of BMP-7 on FSHR and LHR mRNA levels in LGCs

The gene expression of receptor for BMP-7, ALK-6, and BMPR-II was confirmed in LGCs by PCR (Fig. 1A). To investigate the effects of BMP-7 on FSHR mRNA induction in human GCs, the cells were cultured with BMP-7 (100 ng/mL) for 24 h (Fig 1B). Notably, BMP-7 significantly increased FSHR mRNA levels. On the other hand, BMP-7 significantly suppressed LHR mRNA expression (Fig 1C). In

FIGURE 1

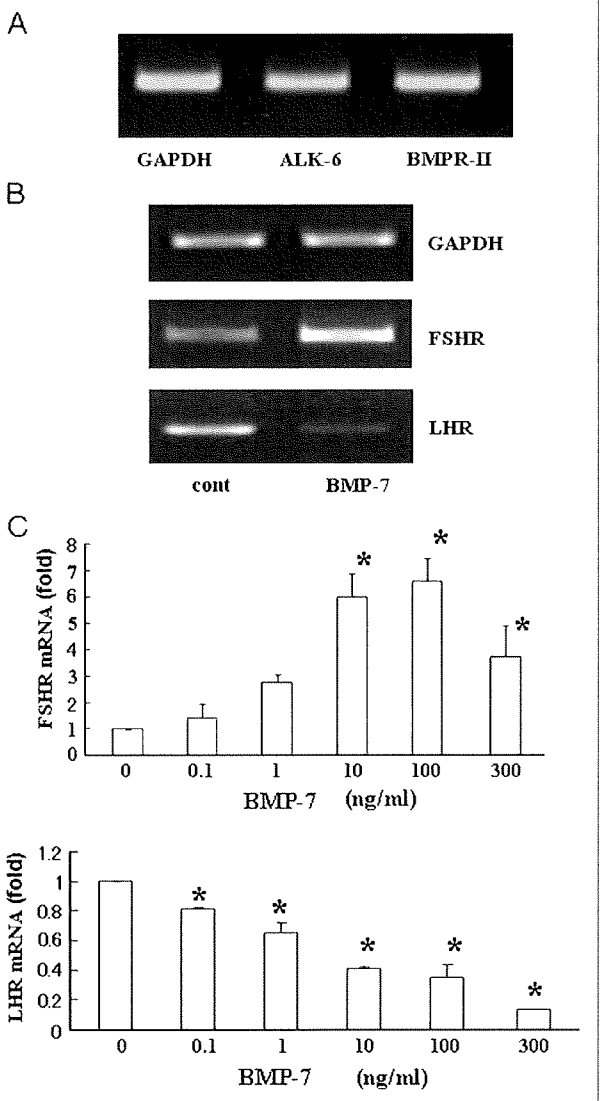

Shi. BMP-7 increases FSH receptor. Fertil Steril 2009.

FIGURE 1 Continued

Expression of bone morphogenetic protein 7 (BMP-7) receptor (BMPR) in human granulosa cells and effect of BMP-7 on FSH receptor (FSHR) mRNA and LH receptor (LHR) mRNA expression. (**A**) The receptor for BMP-7, activin receptor–like kinase (ALK) 6, and BMPR-II in human luteinized granulosa cells (LGCs) were examined with regular polymerase chain reaction (PCR). (**B**) LGCs were cultured with or without BMP-7 (100 ng/mL) for 24 h followed by regular PCR for GAPDH, FSHR, and LHR. (**C**) LGCs were cultured with the indicated concentrations of BMP-7 for 24 h. For the quantification of FSHR and LHR mRNA, real-time PCR analysis was performed and the expression levels of FSHR and LHR mRNA standardized by GAPDH mRNA levels. Data from three different experiments were combined and represented as the mean ± SD relative to an adjusted value of 1.0 for the mean value of the control. *Significant difference at $P<.05$ (vs. control).

a time course study, BMP-7 (100 ng/mL) increased FSHR mRNA levels after 8 h, and the maximal induction of FSHR mRNA expression occurred after 24 h of treatment (Fig. 2). The specificity of BMP-7 was confirmed by the finding that BMP-7–induced FSHR mRNA expression was completely inhibited by an antibody for BMP-7, but not by the control antibody (data not shown).

Induction of FSHR mRNA Expression by BMP-7 was not Via Production of Activins

Activins are known to be a strong inducer of FSHR mRNA expression (9). Therefore, we first examined the mRNA expression levels of inhibin and activin subunits in GCs stimulated with BMP-7. As shown in Fig 3, BMP-7 increased the mRNA levels of inhibin/activin-βA and inhibin/activin-βB, but had no effect on inhibin-α mRNA expression. Based on this finding, we hypothesized that after induction of mRNA for inhibin/activin-β subunits by BMP-7, new activin protein was synthesized, and that this new protein was responsible for inducing FSHR mRNA expression. To determine whether activin or BMP-7 is responsible for the increase in FSHR mRNA, we used SB-431542, an ALK-4, -5, and -7 inhibitor (23) which can selectively inhibit ALK-4, the receptor of activins, but has no effect on ALK-6, the receptor for BMP-7 (12). The LGCs were cultured with BMP-7 (100 ng/mL) or activin-A (100 ng/mL) in the presence or absence of SB-431542 (10 μmol/L). As shown in Figure 4A, SB-431542 significantly suppressed the stimulatory effect of activin-A on FSHR mRNA, whereas SB-431542 had no effect on the up-regulation of FSHR mRNA induced by BMP-7. This finding suggests that although BMP-7 can induce mRNA expression of activin subunits, the BMP-7–induced increase in FSHR mRNA is not mediated by activins. Interestingly, combination of BMP-7 and activin-A did not have an additive effect to increase FSHR mRNA expression, implying some redundancy between the pathways under BMP-7 and activin-A (Fig. 4B).

BMP-7 Treatment Increases Functional FSHR

Cyclic AMP is a well recognized second messenger for activated FSHR. To assess whether FSHR mRNA induction by BMP-7 results in an increase in functional FSHR, LGCs were pretreated with or without BMP-7 (100 ng/mL) for 24 h, and subsequently cultured with 0.1 mmol/L IBMX in the presence or absence of FSH (0.5 IU/mL) for 2 h. As expected, FSH significantly increased cAMP production by LGCs

FIGURE 2

Effect of bone morphogenetic protein 7 (BMP-7) on FSH receptor (FSHR) mRNA expression. Human luteinized granulosa cells (LGCs) were cultured with BMP-7 (100 ng/mL) for different time intervals (3–48 h). Total RNA was then extracted from the LGCs and subjected to real-time polymerase chain reaction to determine the mRNA levels of FSHR. Data were normalized to GAPDH mRNA levels. Solid and open bars represent the relative mRNA levels obtained from the culture in the presence or absence, respectively, of BMP-7. Data from three different experiments were combined and represented as the mean ± SD relative to an adjusted value of 1.0 for the mean value of the each control. *Significant difference at $P<.05$ (vs. control).

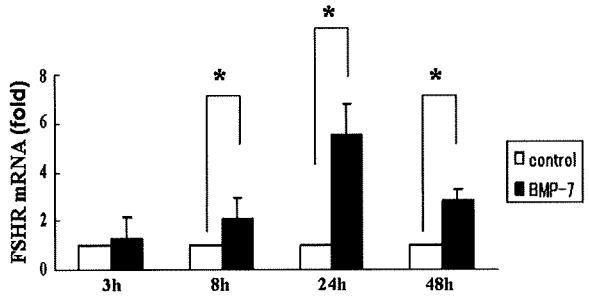

Shi. BMP-7 increases FSH receptor. Fertil Steril 2009.

(Fig. 5). Conversely, BMP-7 pretreatment had no effect on the production of cAMP by LGCs. However, BMP-7 pretreatment significantly enhanced the FSH-induced increase in cAMP levels in LGCs compared with nonpretreatment.

DISCUSSION

The BMP family members are important for folliculogenesis in many species, and there is a growing recognition that BMPs contribute to folliculogenesis by inhibiting luteinization of granulosa cells (12). In the present study, we found that BMP-7 induced FSH receptor (FSHR) mRNA expression in human granulosa cells, suggesting that BMP-7 may contribute to increasing FSH sensitivity of granulosa cells, thus promoting folliculogenesis. Our finding is consistent with that of Lee et al. (18), who, using mouse neonatal ovary, reported that BMP-7 increased FSHR mRNA. On the other hand, BMP-7 treatment inhibited expression of mRNA for LHR, a key factor required by granulosa cells to undergo luteinization (24). Furthermore, we found that the FSHR mRNA induced by BMP-7 resulted in an increase in functional FSHR, as indicated by the finding that FSH stimulated the production of cAMP in BMP-7–primed GCs compared with the control cells.

In the ovary, activins are recognized as important factors in the induction and maintenance of FSHR (7). Our observation

FIGURE 3

Effect of bone morphogenetic protein 7 (BMP-7) on the expression of inhibin/activin-α, inhibin/activin-βA, and inhibin/activin-βB mRNA. Human luteinized granulosa cells (LGCs) were cultured with or without BMP-7 (100 ng/mL) for 24 h. Total RNA was then extracted and subjected to (**A**) regular and (**B**) real-time polymerase chain reaction to determine the mRNA levels of inhibin/activin-α, inhibin/activin-βA, and inhibin/activin-βB. The expression levels of indicated mRNAs were standardized by GAPDH mRNA levels. Data from three different experiments were combined and represented as the mean ± SD relative to an adjusted value of 1.0 for the mean value of the control. *Significant difference at $P<0.05$ (vs. control).

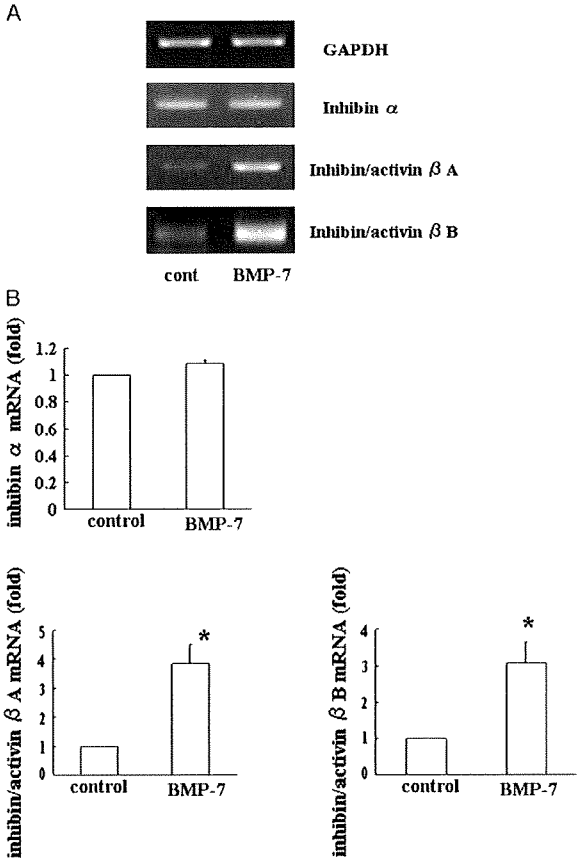

Shi. BMP-7 increases FSH receptor. Fertil Steril 2009.

that BMP-7 increased mRNA levels of not only FSHR but also inhibin/activin-β subunits (Figs. 1 and 3) led us to examine the possibility that the increase in FSHR mRNA might be mediated by an increase in activin protein synthesis. However, SB-431542, an inhibitor of activins but not BMP-7 signaling (23), failed to suppress BMP-7–induced FSHR mRNA expression (Fig. 4A). A possible explanation for this result

FIGURE 4

(**A**) Effect of SB-431542 on activin-A or bone morphogenetic protein 7 (BMP-7)–induced FSH receptor (FSHR) mRNA expression. Human luteinized granulosa cells (LGCs) were cultured with or without BMP-7 (100 ng/mL) or activin-A (100 ng/mL) in the presence or absence of SB-431542 (10 μmol/L), a selective inhibitor of activin receptor–like kinase 4, 5, and 7, for 24 h. Total RNA was then extracted from the LGCs and subjected to real-time polymerase chain reaction (PCR) to determine the mRNA levels of FSHR. Data were normalized to GAPDH mRNA levels. Data from three different experiments were combined and represented as the mean ± SD relative to an adjusted value of 1.0 for the mean value of the control. Bars with different letters indicate a significant difference at $P<.05$. *Significant difference at $P<.05$. NS = not significant. (**B**) LGCs were cultured with BMP-7 (100 ng/mL) and/or activin-A (100 ng/mL) for 24 h, followed by real-time PCR to determine the mRNA levels of FSHR. Data were normalized to GAPDH mRNA levels. Data from three different experiments were combined and represented as the mean ± SD relative to an adjusted value of 1.0 for the mean value of the control. Bars with different letters indicate a significant difference at $P\leq.05$ (b vs. c: $P\leq.02$; c vs. d: $P\leq.01$).

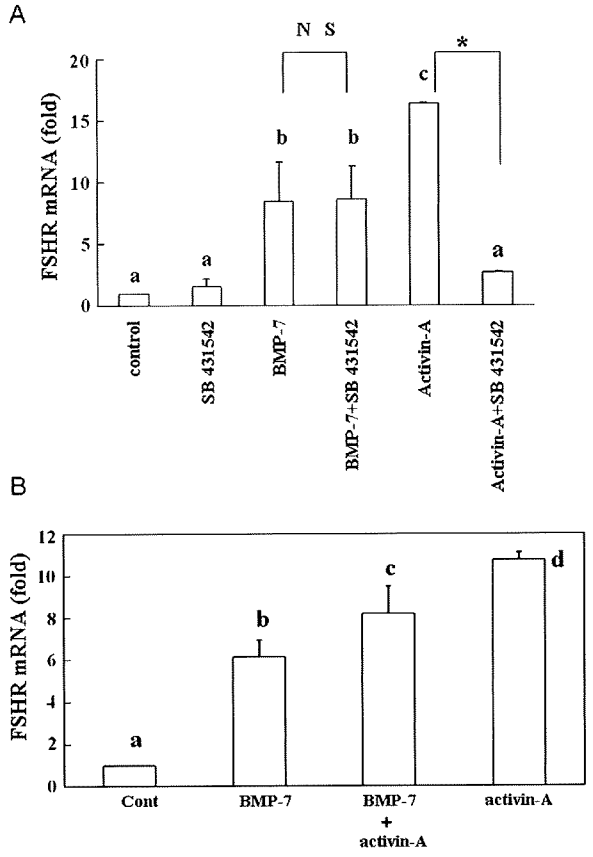

Shi. BMP-7 increases FSH receptor. Fertil Steril 2009.

FIGURE 5

Effect of bone morphogenetic protein 7 (BMP-7) and FSH on cyclic adenosine monophosphate (cAMP) concentration. Human luteinized granulosa cells (LGCs) were cultured with or without BMP-7 (100 ng/mL) for 24 h. The cells were then cultured with 0.1 mmol/L IBMX in the presence or absence of FSH (0.5 IU/mL) for 2 h. The cAMP concentration in the supernatant was measured using a cAMP EIA kit. Data from one representative experiment out of three separate experiments was shown. Results shown are mean ± SD values from quadruplet experimental wells. Bars with different letters indicate a significant difference at $P<.01$ (a vs. b: $P\leq.01$; a vs. c: $P\leq.001$; b vs. c: $P\leq.01$).

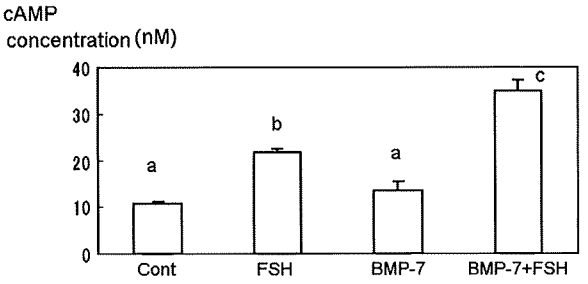

Shi. BMP-7 increases FSH receptor. Fertil Steril 2009.

could be that BMP-7–induced inhibin/activin-β subunits are preferentially recruited to produce inhibin, dimerizing with an inhibin-α subunit that is known to be abundantly expressed in the mature GCs used in this study (25). Thus, it is speculated that BMP-7 and activin-A act on different receptors to increase FSHR mRNA expression. Interestingly, however, combination of BMP-7 and activin-A did not have an additive effect to increase FSHR mRNA expression. Bone morphogenetic protein 7 and activin-A may use redundant signaling pathways downstream of the point affected by SB431542.

Administration of FSH reagent is a standard method for infertility treatment, but many patients are unresponsive to this therapy. Thus, induction of FSHR in growing follicles would be a desirable therapy for infertility patients. Activins have the potential to serve this purpose, because they are recognized as a strong inducer of FSHR. However, because the majority of circulating activins can be bound and inactivated by follistatin (26–28), it appears to be difficult to stimulate ovarian follicles with exogenously administered activins. On the other hand, the relative affinity of follistatin for BMP-7 is less than 1% compared with activins, and the effect of BMP-7 on SMAD phosphorylation in granulosa cells is not reduced in the presence of high doses of follistatin (15). Therefore, BMP-7 would be more suitable than activins for therapeutic use. Notably, the possibility of BMP-7 administration as the new treatment for renal disease has been evaluated by many laboratories (29).

We also found that BMP-7 suppressed LHR expression. Growth and differentiation factor 9, another transforming growth factor (TGF) β superfamily member, also suppresses LHR expression in GCs (30). The present findings suggest that in human GCs, BMP-7 stimulation and inhibition of FSHR and LHR mRNA expression, respectively, may play a role in the course of follicle growth and maturation, in which the increased FSH sensitivity results in induction of folliculogenesis and the decrease in LH sensitivity results in inhibition of ovulation and luteinization. Pangas et al. (24) reported that in an ovarian conditional mouse knockout of *Smad4*, which is a common SMAD for TGF-β superfamily signaling, GCs undergo premature luteinization and express lower levels of FSHR and higher levels of LHR compared with control. Given that BMP-7 also uses the SMAD signaling pathway, the present data appear to be consistent with the description of the *Smad4* knockout mouse.

Abir et al. (17) reported that BMP-7 mRNA is detected only in theca cells of the human ovary, whereas BMP-7 protein is detected in oocytes, GCs, and theca cells. This discrepancy might be due to the cross-reactivity of BMP-7 antibody for other homologous proteins, such as BMP-6. In the present experiment, BMP-7 mRNA was not detected by PCR in granulosa cells, whereas BMP-6 mRNA was amplified abundantly (data not shown). These findings suggest that in human ovaries, as in sheep and mouse (12), BMP-7 expression is primarily localized to the theca cells.

Cultured LGCs used in the present study may not represent the stages of growing follicles. However, our findings that FSHR mRNA levels are clearly up-regulated by BMP-7 in human LGCs are new and open new insights into our understanding of FSHR regulation in the human ovary.

In summary, the present study demonstrated that BMP-7 increased the expression of FSHR mRNA in human GCs, while decreasing LHR mRNA expression. The effect of BMP-7 on FSHR mRNA expression was found to be independent of the effect of activins on FSHR expression. These findings indicate that BMP-7 may play a role in follicular maturation while inhibiting ovulation and luteinization in human ovary, and they identify BMP-7 as a potential treatment for human infertility in patients with a low response to FSH reagent.

Acknowledgments: The authors thank Dr. Heather E. McMahon for her helpful discussion and critical reading of the manuscript and Emi Nose for her excellent technical assistance. They also thank Dr. Shunichi Shimasaki for providing recombinant activin-A protein.

REFERENCES

1. Kumar TR, Wang Y, Lu N, Matzuk MM. Follicle stimulating hormone is required for ovarian follicle maturation but not male fertility. Nat Genet 1997;15:201–4.
2. Kumar TR, Low MJ, Matzuk MM. Genetic rescue of follicle-stimulating hormone beta–deficient mice. Endocrinology 1998;139:3289–95.
3. Erickson GF. Primary cultures of ovarian cells in serum-free medium as models of hormone-dependent differentiation. Mol Cell Endocrinol 1983;29:21–49.
4. Hirshfield AN. Development of follicles in the mammalian ovary. Int Rev Cytol 1991;124:43–101.
5. Kobayashi M, Nakano R, Ooshima A. Immunohistochemical localization of pituitary gonadotrophins and gonadal steroids confirms the "two-cell, two-gonadotrophin" hypothesis of steroidogenesis in the human ovary. J Endocrinol 1991;126:483–8.
6. Yamoto M, Shima K, Nakano R. Gonadotropin receptors in human ovarian follicles and corpora lutea throughout the menstrual cycle. Horm Res 1991;37(Suppl 1):5–11.
7. Minegishi T. Regulation of gonadotropin receptor in the ovary. In: Peter C.K. Leung, Eli Y. Adashi eds. The Ovary. 2nd rev. ed. San Diego: Elsevier, Academic Press, 2004:79–92.
8. Hasegawa Y, Miyamoto K, Abe Y, Nakamura T, Sugino H, Eto Y, et al. Induction of follicle stimulating hormone receptor by erythroid differentiation factor on rat granulosa cell. Biochem Biophys Res Commun 1988;156:668–74.
9. Xiao S, Robertson DM, Findlay JK. Effects of activin and follicle-stimulating hormone (FSH)–suppressing protein/follistatin on FSH receptors and differentiation of cultured rat granulosa cells. Endocrinology 1992;131:1009–16.
10. Richards JS, Ireland JJ, Rao MC, Bernath GA, Midgley AR Jr, Reichert LE Jr. Ovarian follicular development in the rat: hormone receptor regulation by estradiol, follicle stimulating hormone and luteinizing hormone. Endocrinology 1976;99:1562–70.
11. Knecht M, Darbon JM, Ranta T, Baukal AJ, Catt KJ. Estrogens enhance the adenosine 3′,5′-monophosphate–mediated induction of follicle-stimulating hormone and luteinizing hormone receptors in rat granulosa cells. Endocrinology 1984;115:41–9.
12. Shimasaki S, Moore RK, Otsuka F, Erickson GF. The bone morphogenetic protein system in mammalian reproduction. Endocr Rev 2004;25:72–101.
13. Yoshino O, McMahon HE, Sharma S, Shimasaki S. A unique preovulatory expression pattern plays a key role in the physiological functions of BMP-15 in the mouse. Proc Natl Acad Sci U S A 2006;103:10678–83.
14. Shimasaki S, Zachow RJ, Li D, Kim H, Iemura S, Ueno N, et al. A functional bone morphogenetic protein system in the ovary. Proc Natl Acad Sci U S A 1999;96:7282–7.
15. Glister C, Kemp CF, Knight PG. Bone morphogenetic protein (BMP) ligands and receptors in bovine ovarian follicle cells: actions of BMP-4, -6, and -7 on granulosa cells and differential modulation of SMAD-1 phosphorylation by follistatin. Reproduction 2004;127:239–54.
16. Lee WS, Otsuka F, Moore RK, Shimasaki S. Effect of bone morphogenetic protein-7 on folliculogenesis and ovulation in the rat. Biol Reprod 2001;65:994–9.
17. Abir R, Ben-Haroush A, Melamed N, Felz C, Krissi H, Fisch B. Expression of bone morphogenetic proteins 4 and 7 and their receptors IA, IB, and II in human ovaries from fetuses and adults. Fertil Steril 2008;89:1430–40.
18. Lee WS, Yoon SJ, Yoon TK, Cha KY, Lee SH, Shimasaki S, et al. Effects of bone morphogenetic protein-7 (BMP-7) on primordial follicular growth in the mouse ovary. Mol Reprod Dev 2004;69:159–63.
19. Koga K, Osuga Y, Tsutsumi O, Momoeda M, Suenaga A, Kugu K, et al. Evidence for the presence of angiogenin in human follicular fluid and the up-regulation of its production by human chorionic gonadotropin and hypoxia. J Clin Endocrinol Metab 2000;85:3352–5.
20. Osuga Y, Tsutsumi O, Momoeda M, Okagaki R, Matsumi H, Hiroi H, et al. Evidence for the presence of hepatocyte growth factor expression in human ovarian follicles. Mol Hum Reprod 1999;5:703–7.
21. Hirota Y, Osuga Y, Yoshino O, Koga K, Yano T, Hirata T, et al. Possible roles of thrombin-induced activation of protease-activated receptor 1 in human luteinized granulosa cells. J Clin Endocrinol Metab 2003;88:3952–7.
22. Erickson GF, Garzo VG, Magoffin DA. Insulin-like growth factor-I regulates aromatase activity in human granulosa and granulosa luteal cells. J Clin Endocrinol Metab 1989;69:716–24.
23. Inman GJ, Nicolás FJ, Callahan JF, Harling JD, Gaster LM, Reith AD, et al. SB-431542 is a potent and specific inhibitor of transforming growth factor-beta superfamily type I activin receptor–like kinase (ALK) receptors ALK4, ALK5, and ALK7. Mol Pharmacol 2002;62:65–74.

24. Pangas SA, Li X, Robertson EJ, Matzuk MM. Premature luteinization and cumulus cell defects in ovarian-specific *Smad4* knockout mice. Mol Endocrinol 2006;20:1406–22.
25. Knight PG, Glister C. Potential local regulatory functions of inhibins, activins and follistatin in the ovary. Reproduction 2001;121:503–12.
26. Corrigan AZ, Bilezikjian LM, Carroll RS, Bald LN, Schmelzer CH, Fendly BM, et al. Evidence for an autocrine role of activin B within rat anterior pituitary cultures. Endocrinology 1991;28:1682–4.
27. Besecke LM, Guendner MJ, Schneyer AL, Bauer-Dantoin AC, Jameson JL, Weiss J. Gonadotropin-releasing hormone regulates follicle-stimulating hormone-beta gene expression through an activin/follistatin autocrine or paracrine loop. Endocrinology 1996;137: 3667–73.
28. McConnell DS, Wang Q, Sluss PM, Bolf N, Khoury RH, Schneyer AL, et al. A two-site chemiluminescent assay for activin-free follistatin reveals that most follistatin circulating in men and normal cycling women is in an activin-bound state. J Clin Endocrinol Metab 1998;83:851–8.
29. Zeisberg M. Bone morphogenetic protein-7 and the kidney: current concept and open questions. Nephrol Dial Transplant 2006;2:568–73.
30. Elvin JA, Clark AT, Wang P, Wolfman NM, Matzuk MM. Paracrine actions of growth differentiation factor-9 in the mammalian ovary. Mol Endocrinol 1999;13:1035–48.

Human Molecular Genetics, 2010, Vol. 19, No. 3 **480–493**
doi:10.1093/hmg/ddp512
Advance Access published on November 14, 2009

Involvement of a novel preimplantation-specific gene encoding the high mobility group box protein *Hmgpi* in early embryonic development

Mitsutoshi Yamada[1,2], Toshio Hamatani[1,*], Hidenori Akutsu[2], Nana Chikazawa[1,2], Naoaki Kuji[1], Yasunori Yoshimura[1] and Akihiro Umezawa[2]

[1]Department of Obstetrics and Gynecology, Keio University School of Medicine, 35 Shinanomachi Shinjyuku-ku, Tokyo 160-8582, Japan and [2]Department of Reproductive Biology, National Research Institute for Child Health and Development, 2-10-1 Ohkura Setagaya-ku, Tokyo 157-8535, Japan

Received August 24, 2009; Revised October 22, 2009; Accepted November 11, 2009

Mining gene-expression-profiling data identified a novel gene that is specifically expressed in preimplantation embryos. *Hmgpi*, a putative chromosomal protein with two high-mobility-group boxes, is zygotically transcribed during zygotic genome activation, but is not transcribed postimplantation. The *Hmgpi*-encoded protein (HMGPI), first detected at the 4-cell stage, remains highly expressed in pre-implantation embryos. Interestingly, HMGPI is expressed in both the inner cell mass (ICM) and the trophectoderm, and translocated from cytoplasm to nuclei at the blastocyst stage, indicating differential spatial requirements before and after the blastocyst stage. siRNA (siHmgpi)-induced reduction of *Hmgpi* transcript levels caused developmental loss of preimplantation embryos and implantation failures. Furthermore, reduction of *Hmgpi* prevented blastocyst outgrowth leading to generation of embryonic stem cells. The siHmgpi-injected embryos also lost ICM and trophectoderm integrity, demarcated by reduced expressions of Oct4, Nanog and Cdx2. The findings implicated an important role for *Hmgpi* at the earliest stages of mammalian embryonic development.

INTRODUCTION

Preimplantation development encompasses the period from fertilization to implantation. Oocytes cease developing at metaphase of the second meiotic division, when transcription stops and translation is reduced. After fertilization, sperm chromatin is reprogrammed into a functional pronucleus and zygotic genome activation (ZGA) begins, whereby the maternal genetic program governed by maternally stored RNAs and proteins must be switched to the embryonic genetic program governed by *de novo* transcription (1,2). Our previous gene expression profiling during preimplantation development revealed distinctive patterns of maternal RNA degradation and embryonic gene activation, including two major transient 'waves of *de novo* transcription' (3). The first wave during the 1- to 2-cell stage corresponds to ZGA. The second wave during the 4- to 8-cell stage, known as mid-preimplantation gene activation (MGA), induces dramatic morphological changes to the zygote including compaction and blastocele formation, particularly given that few genes show large expression changes after the 8-cell stage. ZGA and MGA together generate a novel gene expression profile that delineates the totipotent state of each blastomere at the cleavage stage of embryogenesis, and these steps are prerequisite for future cell lineage commitments and differentiation. The first such differentiation gives rise to the inner cell mass (ICM), from which embryonic stem (ES) cells are derived, as well as the trophectoderm at the blastocyst stage. However, the molecular regulatory mechanisms underlying this preimplantation development and ES-cell generation from the ICM remain unclear.

Induced pluripotent stem (iPS) cells are ES cell-like pluripotent cells, generated by the forced expression of defined factors in somatic cells, including Pou5f1/Oct4, Sox2, Klf4

*To whom correspondence should be addressed. Tel: +81 353633819; Fax: +81 332261667; Email: t-hama@sc.itc.keio.ac.jp

and Myc (4). These iPS factors are thought to reprogram somatic nuclei in a somewhat similar way as ooplasm does in reconstructed oocytes by nuclear transfer (NT). However, with the exception of Oct4, these factors are not highly expressed maternally in oocytes, and only increased by zygotic transcription during preimplantation, based on expression sequence tag (EST) frequencies in Unigene cDNA libraries and microarray data from oogenesis to preimplantation development (5). Although pluripotency is achieved within 2 days in NT embryos reconstructed with a somatic nucleus, it takes approximately 2 weeks for the establishment of iPS cells. Such immediate induction of pluripotency during preimplantation development is attributed to well-organized transcriptional regulation, i.e. waves of transcription whereby maternal gene products trigger ZGA, which in turn fuels MGA. On the other hand, the forced simultaneous transcription of iPS factors in somatic cells does not efficiently induce these waves of transcription, and it takes a long time to activate the other genes necessary for pluripotency. Studying transcriptional regulation during preimplantation development would therefore also help unravel the establishment of iPS cells as well as pluripotency in these cells.

Large-scale EST projects (6–8) and DNA microarray studies (3,9–11) have revealed many novel genes zygotically expressed during preimplantation development. Very few of these genes, however, are exclusively expressed in preimplantation embryos (12), and such genes ought to have important roles during preimplantation development. For example, *Zscan4*, a novel transcription factor, is expressed specifically in 2-cell stage embryos and a subset of ES cells (13). Reduction of *Zscan4* transcript levels by siRNAs delays progression from the 2-cell to the 4-cell stage, and produces blastocysts that neither implant *in vivo* nor proliferate in blastocyst outgrowth culture. Thus, a transcription factor expressed exclusively in preimplantation embryos is potentially a key regulator of global gene expression changes during preimplantation development. On the other hand, reprogramming gene expression during ZGA and MGA requires considerable changes in chromatin structure (14–16), and modulation of chromatin folding affects access of regulatory factors to their cognate DNA-binding sites. This modulation can be achieved by loosening the chromatin structure, by disrupting the nucleosome structure, by DNA bending and unwinding, and by affecting the strength of DNA-histone interactions via postsynthetic modifications of histones (17,18). Many of these structural changes are mediated by a large and diverse superfamily of high-mobility-group (HMG) proteins, which are the second most abundant chromosomal proteins after histones (18).

This study identified a novel preimplantation-specific gene, *Hmgpi*, which encodes a chromosomal protein containing HMG box domains. It reports a detailed expression analysis of *Hmgpi* and the *Hmgpi*-encoded protein (HMGPI), which was translocated from the cytoplasm to nuclei at the blastocyst stage. Loss-of-function studies were also conducted using siRNA technology. The siRNA-induced reduction in *Hmgpi* expression caused developmental loss at preimplantation stages and hampered implantation through reduced proliferation of both ICM-derived cells and trophectodermal cells during peri-implantation development.

RESULTS

Gene structure of a preimplantation-stage-specific gene, *Hmgpi*

In silico analysis identified *Hmgpi* (an **HMG**-box protein, **p**reimplantation-embryo-specific) as a preimplantation-stage-specific gene encoding a chromosomal protein containing HMG box domains. The *Hmgpi* transcript levels are probably upregulated during ZGA (1- to 2-cell stages) to peak at the 4-cell stage, based on gene expression profiling (3,9) (Fig. 1A). Using the public expressed-sequence tag (EST) database, 16 cDNA clones were found exclusively in preimplantation-embryo libraries (2- to 8-cell stages) (Fig. 1B). One of these contained the full *Hmgpi* gene coding sequence (AK163257) (Fig. 1C), spanning 2579 bp and split into two exons, which encode a protein of 394 amino acids (aa) (NP_001028965) harboring a SANT domain ('SWI3, ADA2, N-CoR, and TFIIIB' DNA-binding domain) and two HMG-box domains, based on SMART domain prediction analysis (19) (Fig. 1C). In the NCBI Gene database, the *Hmgpi* gene is called Ubtf-like 1 (*Ubtfl1*) based on aa sequence similarity (36% identity and 58% positives by BLAST) to *Ubtf*-encoded protein 'upstream binding transcription factor', which contains a SANT domain and six HMG-box domains. Two rat homologs (*Ubtfl1* and *RGD1304745*) and three human homologs (*UBTFL1-3*) of the mouse *Hmgpi* were identified by BLASTing of NP_001028965 against the NCBI nucleotide database. Pairwise alignment scores by BLAST of amino acid sequences for rat and human homologs are 72.3–72.5% and 53.8–54.1%, respectively (Fig. 1D and Supplementary Material, Table S1), while those for nucleotide sequences are 83.7 and 66.8–67.0%, respectively. All these human homologs were predicted by *in silico* genome-based analysis, and have no ESTs in the Unigene database. The absence of human ESTs may reflect the paucity of cDNA libraries of human preimplantation embryos in the Unigene database, despite specific expression of the Hmgpi gene in human preimplantation embryos. Based on the number and the type of HMG-box domains, this novel protein could also be categorized into the HMG-box family (HMGB). A dendrogram of aa sequence similarity in HMG family proteins indicates two HMG subgroups (Fig. 1E). One includes the HMG-nucleosome binding family (HMGN) and the HMG-AT-hook family (HMGA), and the other is HMGB that includes HMGPI. All members of HMGB contain two HMG-box domains ('HMG-box' or 'HMG-UBF_HMG-box').

Expression of the *Hmgpi* gene and protein

First, we experimentally confirmed the preimplantaion-stage-specific expression pattern of *Hmgpi* suggested by the *in silico* analysis. Northern blot analysis using a mouse multiple tissue poly(A)RNA panel (FirstChoice® Mouse Blot 1 from Ambion, Austin, TX, USA) failed to detect expression of the *Hmgpi* gene (data not shown). While RT–PCR analysis using cDNA isolated from mouse adult tissues and fetuses (E7, E11, E15 and E17) also failed to show *Hmgpi* expression, RT–PCR analysis for preimplantation embryos indicated *Hmgpi* expression from the 2-cell embryo to the blastocyst

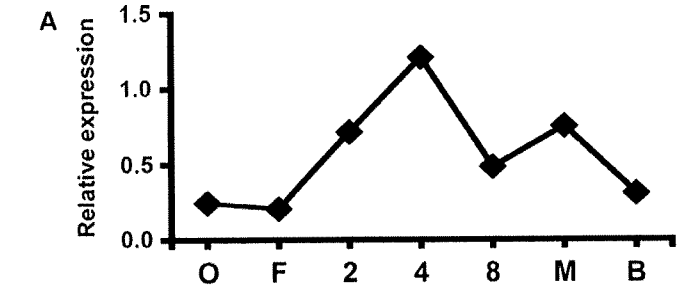

B

Developmental stage	Gene EST	Total EST in pool
Oocyte	0	19488
Unfertilized ovum	0	20366
Zygote	0	28382
Cleavage	16	65852
Blastocyst	0	69938
Egg cylinder	0	12257
Gastrula	0	28673
Organogenesis	0	128591
Fetus	0	670244
Neonate	0	107177
Juvenile	0	293396
Adult	0	1026072

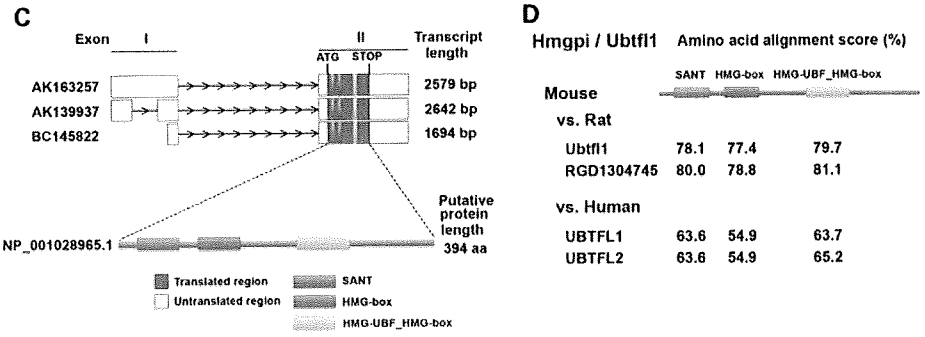

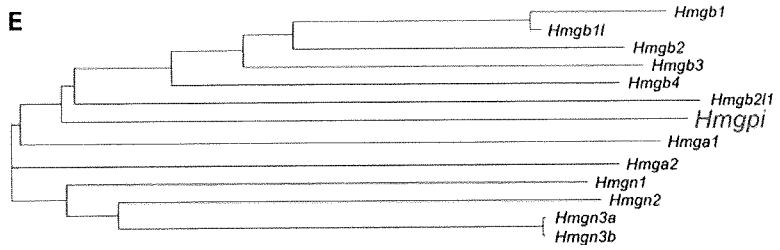

Figure 1. *In silico* analysis of *Hmgpi* expression. (**A**) Previous microarray analysis of *Hmgpi* expression. *Hmgpi* expression appeared at the 2-cell stage, peaked at the 4-cell stage and then decreased (3). (**B**) Expression sequence tag (EST) frequencies in Unigene cDNA libraries. Out of 4.7 million mouse ESTs, 16 *Hmgpi* clones were exclusively detected at the cleavage stages: 9, 2 and 5 ESTs from 2-cell, 4-cell and 8-cell libraries, respectively. (**C**) Exon–intron structures and a putative protein structure of *Hmgpi*. *Hmgpi* has three exon–intron models and one protein model. Predicted protein domains are also shown. (**D**) Conserved domains of *Hmgpi/Ubtfl1* gene in mouse, rat and human. Pairwise alignment scores of conserved domains between species were shown. (**E**) Phylogenetic tree of gene nucleotide acid sequences containing HMG domains determined by a sequence distance method and the neighbour-joining (NJ) algorithm (41) using Vector NTI software (Invitrogen, Carlsbad, CA, USA).

stage (Fig. 2A). Furthermore, significant expression of *Hmgpi* was detected in ES cells, although not in embryonic carcinoma (EC) cells nor in mesenchymal stem cells (Fig. 2B). The relative abundance of *Hmgpi* transcripts in preimplantation embryos was measured by real-time quantitative RT–PCR (qRT–PCR) analysis (Fig. 2C). Four independent experiments were conducted with four replicates of 10 embryos each. To normalize the qRT–PCR reaction efficiency, *H2afz* was used as an internal standard (20). *Hmgpi* mRNA levels increased during the 1- to 2-cell stage, peaked at the 4-cell stage, and then gradually decreased during the 8-cell to blastocyst stage (Fig. 2C). The *in silico*-predicted preimplantation-stage-specific expression pattern of *Hmgpi* was therefore validated.

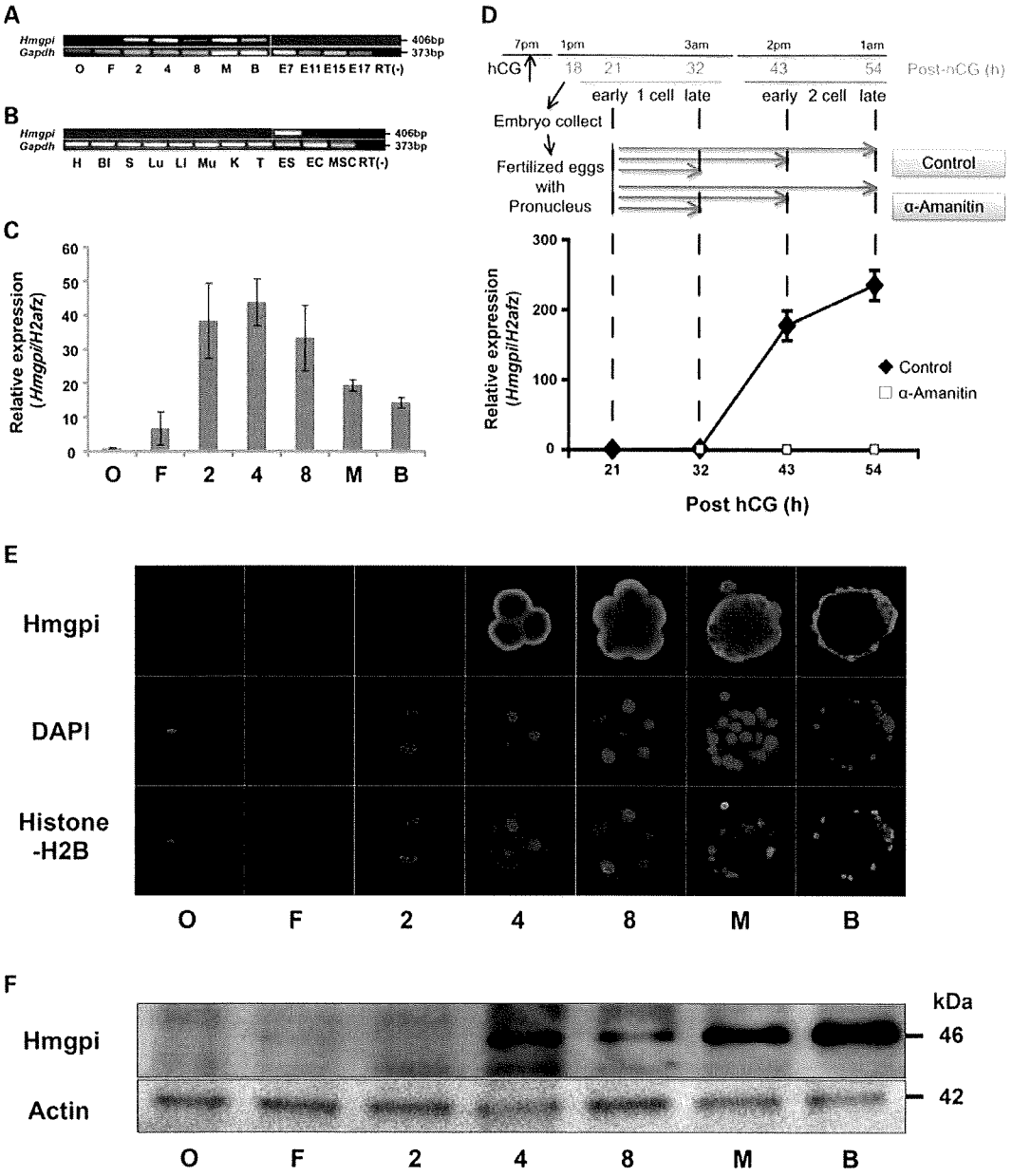

Figure 2. Expression of *Hmgpi* in preimplantation embryos and other tissues. (**A**) RT–PCR analysis of *Hmgpi* expression during preimplantation and postimplantation development (E7–E17). Three sets of 10 pooled embryos were collected from each stage (O: oocyte, F: fertilized egg, 2: 2-cell embryo, 4: 4-cell embryo, 8: 8-cell embryo, M: morula, and B: blastocyst) and used for RT–PCR analysis. The predicted sizes of the PCR products of *Hmgpi* and *Gapdh* are 406 and 373 bp, respectively. No PCR products were detected in the no-RT negative control (4-cell embryo). (**B**) RT–PCR analysis of *Hmgpi* expression in adult tissues, ES cells, EC cells and mesenchymal stem cells. mRNA was isolated from mouse tissues (H: heart, Bl: bladder, S: spleen, Lu: lung, Li: liver, Mu: muscle, K: kidney, T: testis, ES: ES cells, EC: EC cells, and MSC: mesenchymal stem cells). No PCR products were detected in the no-RT negative control (ES cells). (**C**) Real-time quantitative RT–PCR analysis of *Hmgpi* expression during preimplantation development. Fold differences in amounts of *Hmgpi* mRNA from the same numbers of oocytes (O), fertilized eggs (F), 2-cell embryos (2), 4-cell embryos (4), 8-cell embryos (8), morulae (M) and blastocysts (B) are shown after normalization to an internal reference gene (mouse *H2afz*). Values are means ± SE from four separate experiments. (**D**) *De novo* (zygotic) transcription of the *Hmgpi* gene. α-Amanitin studies revealed that *Hmgpi* is transcribed zygotically, but not maternally. *Hmgpi* expression was not observed before the 2-cell stage and α-amanitin completely inhibited *de novo* transcription at the 2-cell stage (closed rhombus: control group, open square: α-amanitin-treated group). The expression levels were normalized using *H2afz* as a reference gene. Values are means ± SE from four separate experiments. (**E**) Immunocytochemical analysis of HMGPI expression. MII oocytes and preimplantation embryos were immunostained with an anti-HMGPI antibody (red) and an anti-Histone-H2B antibody as a positive control of nuclear staining (green). Nuclei are shown by DAPI staining (blue). HMGPI protein was detected from 4-cell embryos to blastocysts. (**F**) Immunoblot analysis of HMGPI during preimplantation development. An amount of extracted protein corresponding to 100 oocytes or embryos was loaded per lane. Actin was used as a loading control. The representative result is shown from three independent experiments.

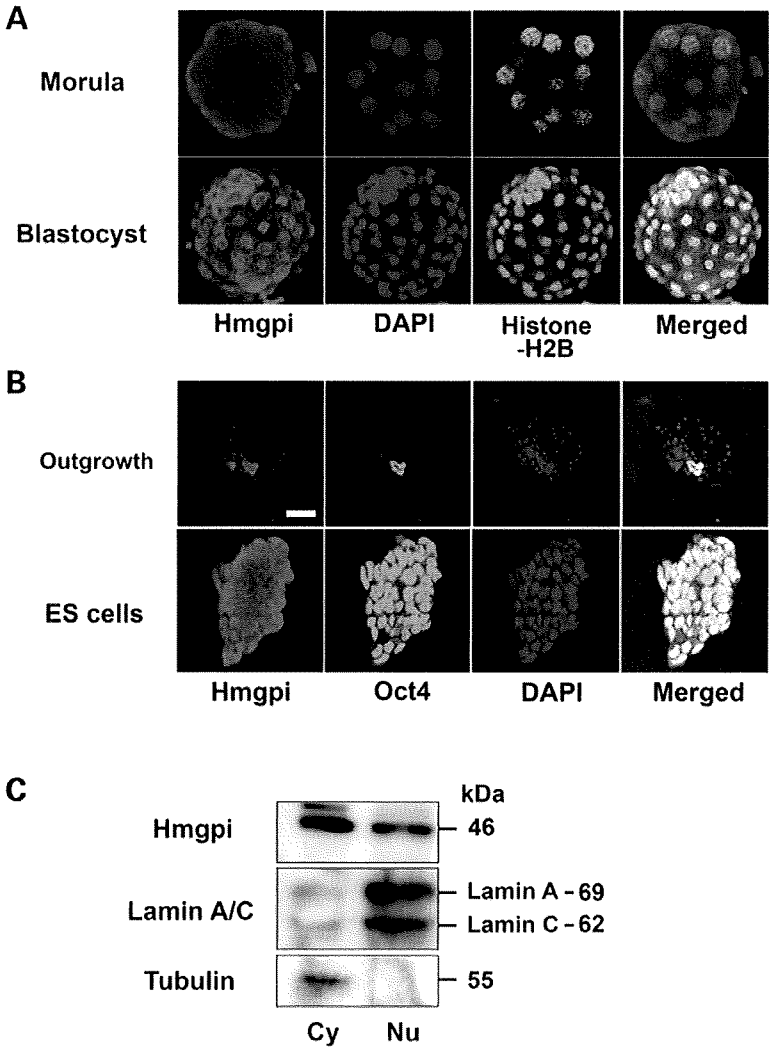

Figure 3. Localization of HMGPI in preimplantation embryos. (**A**) Nuclear translocation of HMGPI protein at the blastocyst stage. HMGPI was mainly detected in the cytoplasm of preimplantation embryos (from 4-cell embryos to morulae), but in the nuclei of blastocysts. Nuclei are shown by immunostaining with an anti-Histone-H2B antibody (green) and DAPI staining (blue). (**B**) Confocal microscopy images of blastocyst outgrowth and ES cells stained with antibodies to *Hmgpi* and *Oct4*, and with DAPI. Scale bar = 50 μM. (**C**) Western blotting analysis of HMGPI in cytoplasmic (Cy) and nuclear (Nu) fractions of ES cells. Lamin A/C and tubulin were used as markers of the nuclear and cytoplasmic fractions, respectively.

We then performed qRT–PCR analysis using α-amanitin to investigate *de novo* (zygotic) transcription of the *Hmgpi* gene. The supplementation of α-amanitin during *in vitro* culture from the 1-cell stage significantly reduced *Hmgpi* mRNA expression in the 2-cell embryos at post-hCG 43 and 53 h (early and late 2-cell stage, respectively) (Fig. 2D), implying that *Hmgpi* is transcribed zygotically during the major burst of ZGA, but not maternally.

To study the temporal and spatial expression pattern of the *Hmgpi*-encoded protein (HMGPI), we raised a polyclonal antibody against *Hmgpi* peptides. Western blot analysis of extracts from the mouse blastocysts showed only a single band corresponding to 46 kDa detected by the anti-HMGPI antibody. In addition, preincubation with the HMGPI peptide antigen abolished detection of the HMGPI protein, while preincubation with a control peptide had no effect on the immunodetection (Supplementary Material, Fig. S1). Although *Hmgpi* transcription started at the 2-cell stage, peaked at the 4-cell stage and then gradually decreased until the blastocyst stage (Fig. 2C), immunostaining and immunoblotting analysis revealed HMGPI expression from the 4-cell stage until the blastocyst stage, indicating a delayed expression pattern of HMGPI compared with that of the *Hmgpi* transcript. It was also notable that both ICM cells and trophectodermal cells retained HMGPI expression in blastocysts.

On the other hand, immunostaining for HMGPI in preimplantation embryos showed a unique subcellular localization pattern. Although a putative nuclear protein due to its role

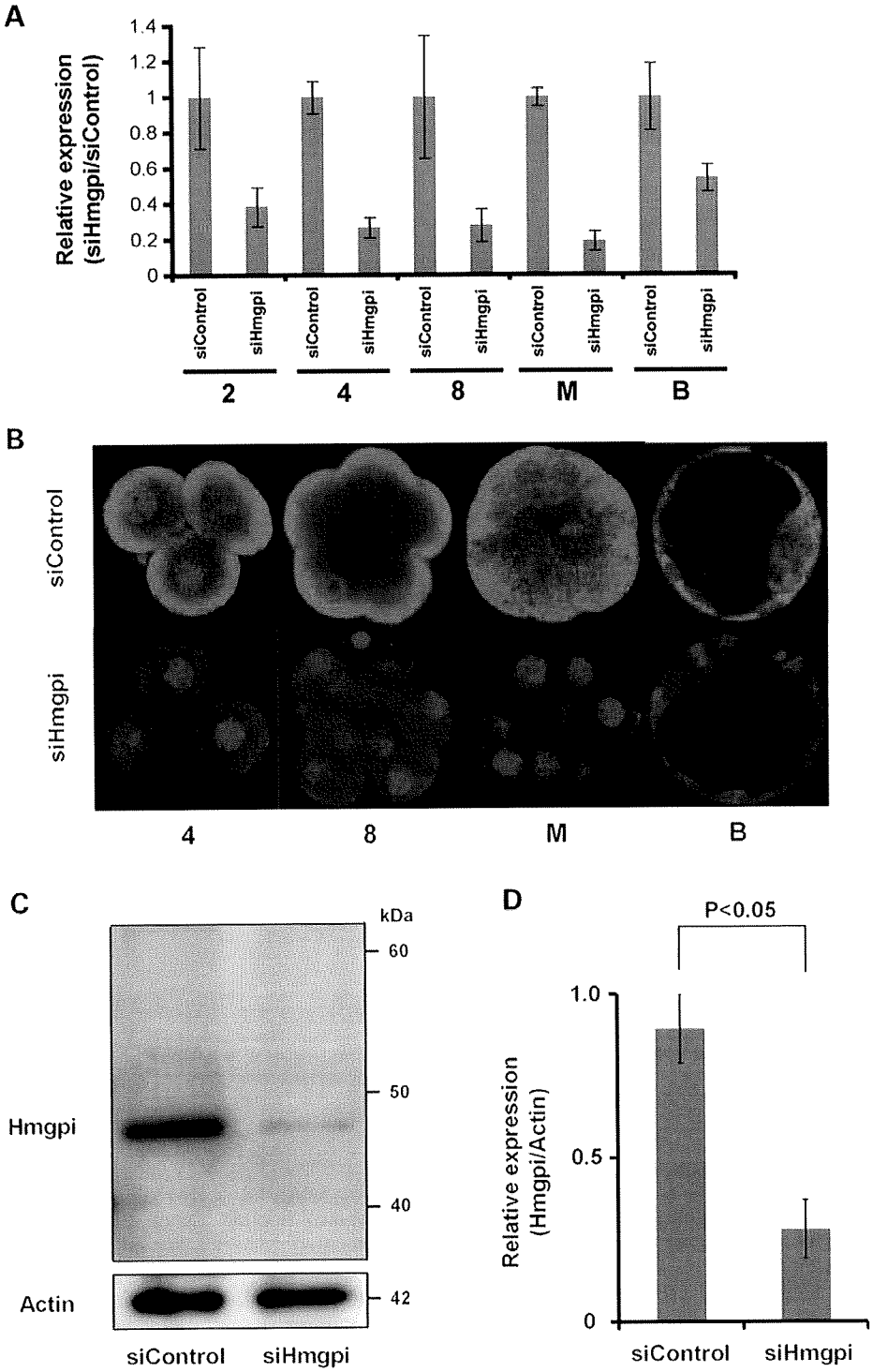

Figure 4. Loss-of-function study by siRNA technology. (**A**) Transcript levels of *Hmgpi* in embryos injected with control siRNA (siControl) and *Hmgpi* siRNA (siHmgpi) by real-time quantitative RT–PCR analysis. The expression levels were normalized using *H2afz* as a reference gene. Values are means ± SE for four separate experiments. (**B**) Laser scanning confocal microscopy images of HMGPI protein expression in a 4-cell embryo, 8-cell embryo, morula and blastocyst after injection with siControl or siHmgpi (red, HMGPI; blue, chromatin). (**C** and **D**) Immunoblot analysis of HMGPI expression at the blastocyst stage in siControl-injected and siHmgpi-injected embryos. The relative amount of HMGPI (46 kDa) was determined at the blastocyst stage (left: siControl-injected embryos, right: siHmgpi-injected embryos). The expression levels were normalized using actin expression (42 kDa) as a reference. Values are means ± SE from three separate experiments.

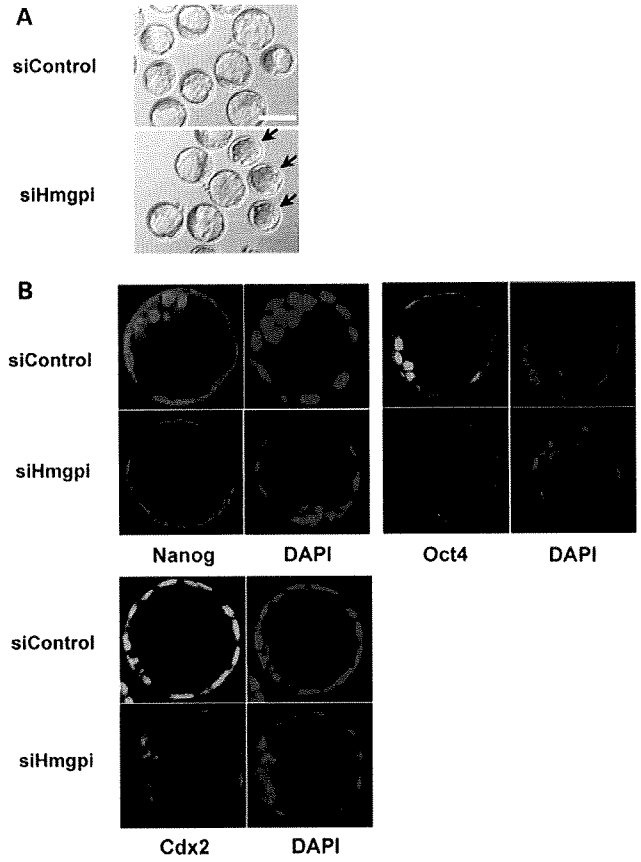

Figure 5. Function of *Hmgpi* in preimplantation development. (**A**) A pair of representative photos showing the development of embryos injected with *Hmgpi* siRNA (siHmgpi) and Control siRNA (siControl). The siHmgpi-injected embryos arrested at the morula stage are indicated by arrows. Scale bar = 100 μM. (**B**) For Nanog, Oct4 and Cdx2 immunostaining, all blastocysts in the siHmgpi-injected and siControl-injected groups were processed simultaneously. The laser power was adjusted so that the signal intensity was below saturation for the developmental stage that displayed the highest intensity and all subsequent images were scanned at that laser power. This allowed us to compare signal intensities for Nanog, Oct4 and Cdx2 expression between the siHmgpi-injected and siControl-injected embryos (Supplementary Material, Table S2).

as a transcription factor, HMGPI was detected mainly in the cytoplasm without any evidence of a nuclear localization from the 4-cell to the morula stage, suggesting a role other than transcriptional regulation (Fig. 2E). In contrast, HMGPI was localized to the nuclei rather than to the cytoplasm of blastocysts (Figs 2E and 3A). During blastocyst outgrowth, HMGPI was expressed in the nuclear region of most outgrowing cells, with scant amounts detected in the cytoplasm (Fig. 3B). Interestingly, Oct4-positive cells derived from the ICM showed particularly strong positive staining for HMGPI in the nucleus, suggesting a specific role as a nuclear protein in ES cells (Fig. 3B). On more closely examining HMGPI in ES cells, we found that almost all the Oct4-positive undifferentiated ES cells in a colony also expressed HMGPI (Fig. 3B), and immunoblotting confirmed HMGPI expression in both nuclear and cytoplasmic fractions of ES cells (Fig. 3C).

Effect of siRNA on *Hmgpi* mRNA level and protein synthesis

To investigate a role of *Hmgpi* in early embryonic development, we knocked down *Hmgpi* expression in mouse preimplantation embryos. We employed an oligonucleotide-based siRNA (denoted here siHmgpi and obtained from PE Applied Biosystems, Foster City, CA, USA). Zygotes injected with *Hmgpi* siRNAs (siHmgpi) or control siRNA (siControl) and non-injected zygotes as negative controls were cultured. *Hmgpi* expression was severely suppressed in the siHmgpi-injected embryos, and significantly lower than those in the siControl-injected or non-injected embryos (Fig. 4A). The siControl-injected embryos did not show any difference from the non-injected embryos in *Hmgpi* expression (data not shown). In addition, immunofluorescent staining clearly demonstrated that the siRNA injection reduced HMGPI protein expression in an individual preimplantation embryo (Fig. 4B). In the same set of experiments, the HMGPI levels were also assayed by western blotting (Figs 4C and 4D). HMGPI expression was significantly reduced in siHmgpi-injected blastocysts (0.89 ± 0.10) compared with that in negative controls (0.28 ± 0.08; $P < 0.05$).

Furthermore, we confirmed that siHmgpi had no influence on the expression of other genes with sequence similarities to *Hmgpi*, namely *Ubtf*, *Hmgb1*, *Hmgb2* and *Hmgb3*. Although *Ubtf*, *Hmgb1*, *Hmgb2* and *Hmgb3* were all expressed in control preimplantation embryos, the siHmgpi construct used in this study did not affect the expression of these genes in the siHmgpi-injected embryos (Supplementary Material, Fig. S2). On the other hand, it has been demonstrated that loss-of-function of these genes produces no distinct phenotypes at the pre- and peri-implantation stages (21).

Effect of *Hmgpi* siRNA on preimplantation development

To study the function of *Hmgpi* during preimplantation development, siHmgpi-injected or siControl-injected zygotes were cultured *in vitro* until the blastocyst stage. The embryos injected with siHmgpi at 21–23 h after hCG administration often failed to become blastocysts at 3.5 days postcoitum (dpc) (Fig. 5A). In addition, the reduction in Hmgpi expression significantly suppressed preimplantation development, whereby $68.9 \pm 1.3\%$ of siHmgpi-injected embryos became blastocysts, while $94.1 \pm 1.3\%$ of siControl-injected embryos reached the blastocyst stage (Supplementary Material, Fig. S3; $P < 0.0001$). Most of the siHmgpi-injected embryos that failed to become blastocysts showed developmental arrest after the morula stage and did not appear to form blastocoels, suggesting impairment of trophectodermal development (Supplementary Material, Fig. S3). To analyze the phenotype of siHmgpi-injected embryos further, we performed immunofluorescence staining of lineage-specific markers such as Cdx2, Nanog and Oct4 at the blastocyst stage. Although siHmgpi-injected embryos that reached the blastocyst stage appeared morphologically intact, the expression of lineage-specific markers was reduced (Fig. 5B). Cdx2, which is required for implantation and extra-embryonic development, was particularly and markedly down-regulated in trophectodermal cells, while Nanog and Oct4

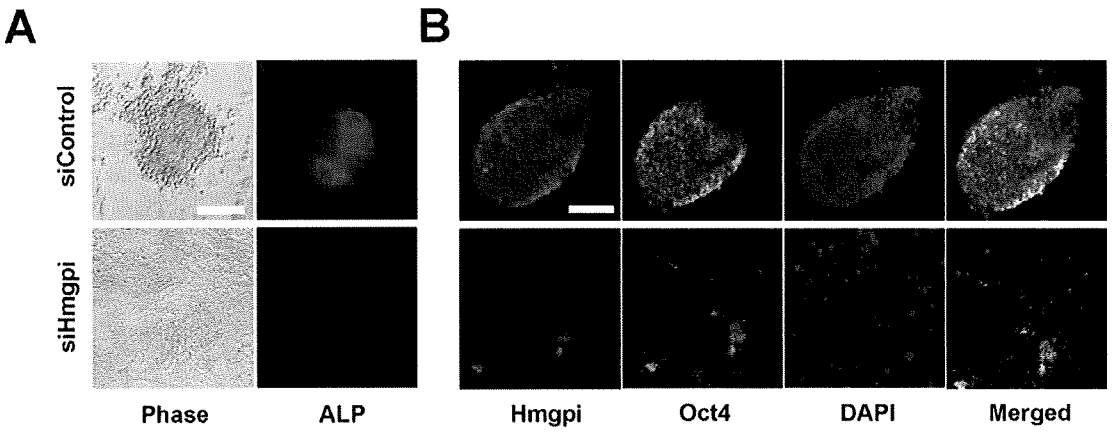

C

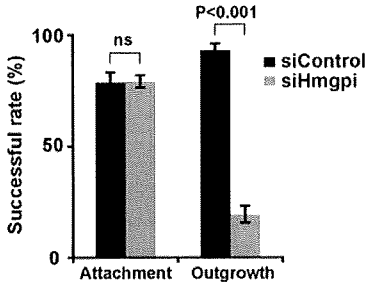

	Tested blastocysts	Attachment (%)	Outgrowth (%)
siControl	51	34 (66.6)	30 (88.2)
siHmgpi	20	15 (75.0)	2 (13.3)
siControl	117	92 (78.6)	80 (86.9)
siHmgpi	13	10 (76.9)	2 (20.0)
siControl	55	49 (89.0)	48 (97.9)
siHmgpi	8	7 (87.5)	1 (14.2)
siControl	41	33 (80.4)	33 (100.0)
siHmgpi	13	10 (76.9)	3 (30.0)

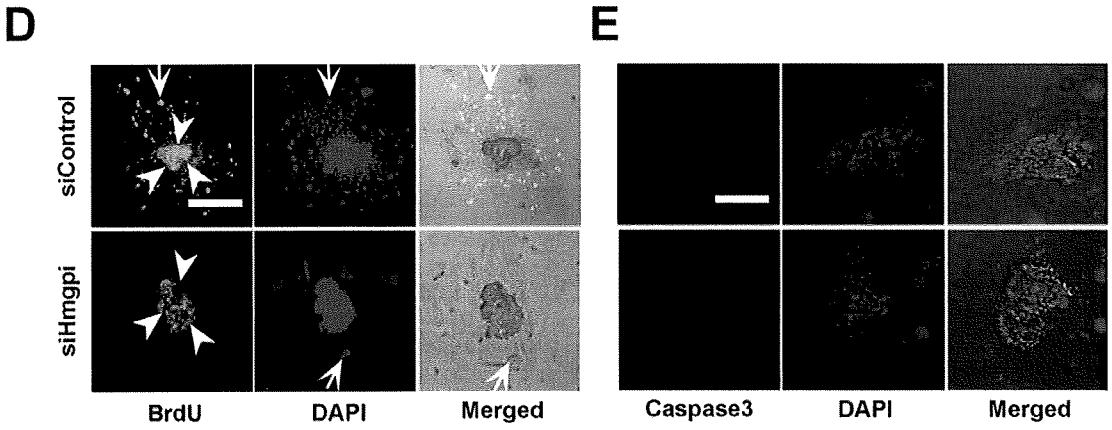

F

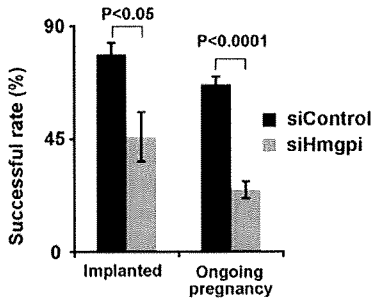

	Transferred embryos	Implanted (%)	Ongoing pregnancy (%)
siControl	30	23 (76.7)	20 (66.7)
siHmgpi	18	6 (33.3)	3 (16.7)
siControl	30	25 (83.3)	18 (60.0)
siHmgpi	32	20 (62.5)	10 (31.2)
siControl	16	13 (81.2)	12 (75.0)
siHmgpi	24	15 (62.5)	7 (29.1)
siControl	20	13 (65.0)	13 (65.0)
siHmgpi	32	8 (25.0)	7 (21.8)

were likewise downregulated in ICM cells of the siHmgpi-injected embryos (Fig. 5B and Supplementary Material, Table S2). Thus, *Hmgpi* is essential for the earliest embryonic development; both ICM and trophectodermal development.

Effect of *Hmgpi* siRNA on *in vivo* and *in vitro* peri-implantation development

To investigate the role of *Hmgpi* in proliferation of the ICM and trophectodermal cells, siHmgpi-injected and siControl-injected embryos were further cultured *in vitro* from the blastocyst stage, and attachment and outgrowth of each embryo on gelatin-coated culture plates was examined. HMGPI expression in siHmgpi-injected embryos was significantly reduced, and immunostaining showed that many colonies of ICM cells in the embryos collapsed during outgrowth culture (Fig. 6A and B). Although the vast majority of ICMs from siControl-injected embryos showed successful attachment (80.3 $\pm$ 4.9%) and vigorous outgrowth (96.2 $\pm$ 2.7%), those from siHmgpi-injected embryos failed to proliferate or produced only a residual mass (19.3 $\pm$ 3.8%) despite successfully attaching (79.0 $\pm$ 2.8%) (Fig. 6C; attachment ns; outgrowth, $P < 0.001$). These results implied that *Hmgpi* is essential for proliferation of ICM and trophectodermal cells in peri-implantation development, and for derivation of ES cells.

We then investigated cell proliferation and apoptosis during blastocyst outgrowth. Comparable incorporation of BrdU in blastocyst outgrowths of siHmgpi-injected embryos was less than that of siControl-injected embryos. Proliferation was significantly reduced in ICM-derived cells and dramatically suppressed in trophoblast cells (Fig. 6D). Embryonic fibroblasts were used as a feeder layer in this study and could support ICM cells, thus proliferation should have proceeded regardless of trophectodermal cell support. Therefore, the collapsed ICM-derived colonies in the current experiment were not a secondary effect of reduced proliferation in trophoblast cells, but a direct effect of the siHmgpi-induced decrease in ICM proliferation. Apoptosis was not detected in any cells during blastocyst outgrowth of siHmgpi-injected embryos, based on the absence of active caspase3 (Fig. 6E). Taken together, these findings show that *Hmgpi* is indispensable for proliferation of the ICM and trophectodermal cells in peri-implantation development and for the generation of ES cells.

Finally, we tested whether the experimental blastocysts could develop *in vivo* by transferring siHmgpi-injected and siControl-injected blastocysts into the uterus of pseudopregnant mice. Only 45.8 $\pm$ 9.7 and 24.7 $\pm$ 3.3% of blastocysts injected with siHmgpi implanted and developed, respectively, whereas most of the siControl-injected embryos showed successful implantation and ongoing development (76.5 $\pm$ 4.0 and 66.6 $\pm$ 3.3%, respectively) (Fig. 6F; implanted, $P < 0.05$; ongoing pregnancy, $P < 0.0001$). These results confirmed a role for *Hmgpi* in peri-implantation embryonic development.

DISCUSSION

We previously analyzed the dynamics of global gene expression changes during mouse preimplantation development (3). Understanding these preimplantation stages is important for both reproductive and stem cell biology. Many genes showing wave-like activation patterns (e.g. ZGA and MGA) during preimplantation were identified, and any or all of these may contribute to the complex gene regulatory networks. *Hmgpi*, one of the few novel preimplantation-specific genes, is involved in early development, implantation and ES cell derivation.

Structure-based prediction of *Hmgpi* function

Structural information about a protein sometimes hints at functional mechanisms, which remain unknown for *Hmgpi*'s clear role in early embryonic development. The HMG family proteins are abundant nuclear proteins that bind to DNA in a non-sequence-specific manner, influence chromatin structure and enhance the accessibility of binding sites to regulatory factors (17). Based on the number and the type of HMG domains, *Hmgpi* is relevant to the HMGB subfamily, characterized by containing two HMG-box domains ('HMG-box' or 'HMG-UBF_HMG-box'), rather than either the HMGA or HMGN subgroups. *Hmgpi* is also known as *Ubtfl1* in the NCBI gene database, based on sequence similarity to *Ubtf*, a well-known ZGA gene (3,22). *Ubtf*, encoding a SANT domain and six HMG-box domains, functions exclusively in RNA polymerase I (Pol I) transcription (23) and acts through its multiple HMG boxes to induce looping of DNA, which creates a nucleosome-like structure to modulate tran-

Figure 6. Function of *Hmgpi* in peri-implantation development. (**A**) Blastocyst outgrowth and alkaline phosphatase (AP) activity in the siHmgpi-injected and siControl-injected embryos, carried out according to a standard procedure (42). Representative images of phase-contrast microscopy for blastocyst outgrowth and fluorescent immunocytochemistry for AP are shown. Scale bar = 100 μM. (**B**) Confocal microscopy images of blastocyst outgrowth for the siHmgpi-injected and siControl-injected embryos, stained with antibodies to Hmgpi and Oct4. Nuclei are shown by DAPI staining. Scale bar = 100 μM. (**C**) Successful rate of blastocyst outgrowth for siHmgpi-injected and siControl-injected embryos. Successful outgrowth in this assay was indicated by the presence of proliferating cells after 6 days in culture. The experiment was repeated four times. (**D**) BrdU incorporation assay for blastocyst outgrowth of the siHmgpi-injected and siControl-injected embryos. Cell proliferation was determined by BrdU incorporation (ICM: arrowhead, trophectodermal cells: arrow). The trophectodermal component contained few cells and BrdU incorporation was confined to the ICM core; however, cell proliferation was reduced in the blastocyst outgrowth of siHmgpi-injected embryos compared with that of the siControl-injected embryos. Nuclei are shown by DAPI staining. Scale bar = 100 μM. (**E**) Immunocytochemistry with an anti-caspase3 antibody in blastocyst outgrowth of the siHmgpi-injected and siControl-injected embryos. Apoptotic cells were not apparent in the blastocyst outgrowth of either injected embryo. Nuclei are shown by DAPI staining. Scale bar = 100 μM. (**F**) Successful rate of siHmgpi-injected and siControl-injected embryo transfer. We transferred 3.5 dpc blastocysts into the uteri of 2.5 dpc pseudopregnant ICR female mice. The pregnant ICR mice were sacrificed on day 12.5 of gestation and the total numbers of implantation sites and of live and dead embryos/fetuses were counted. The experiment was repeated four times.

scription of the 45S precursor of ribosomal RNA (rRNA) by Pol I (24,25). Because the association of UBTF with rRNA genes *in vivo* is not restricted to the promoter and extends across the entire transcribed portion, UBTF promotes the formation of nucleolar organizer regions, indicative of 'open' chromatin (26). Based on the sequence similarity between UBTF and HMGPI, HMGPI might also bind to DNA in a non-specific manner, and modulate chromatin during peri-implantation when dynamic chromatin change is essential.

Alternatively, HMGPI may act as a cytokine during preimplantation development in a similar manner to HMGB1. HMGB proteins are found primarily in the cell nucleus, but also to varying extents in the cytosol (27,28), and have been suggested to shuttle between compartments (17). HMGB1 is indeed passively released from nuclei upon cell death and actively secreted as a cytokine (29), and the addition of recombinant HMGB1 into culture medium enhances *in vitro* development of mouse zygotes to the blastocyst stage in the absence of BSA supplementation (30). Although HMGPI failed to be detected in culture media after *in vitro* culture of preimplantation embryos or ES cells in this study (data not shown), two different modes of Hmgpi action, chromatin modulator and secreted mediator, should be taken into consideration as discussed later.

Role of *Hmgpi* during peri-implantation

The HMGPI protein was first detected in 4-cell embryos and then abundantly expressed in 8-cell embryos, morulae, ICM, trophectoderm and ES cells. Although *Hmgpi* transcription peaked at the 4-cell stage, the most dramatic siRNA effect appeared at the blastocyst and subsequent stages. This discrepancy between temporal expression and phenotype is attributed to three possible mechanisms. First, protein expression is generally delayed from transcription, indicated here by the *Hmgpi* transcripts and HMGPI protein expression peaking at the 4-cell stage and blastocyst stage, respectively. Similarly, *Stella* (31) and *Pms2* (32) are maternal-effect genes, but do not cause developmental loss until later preimplantation stages. A second possibility is the incompleteness of siRNA knockdown. One limitation of such knockdown experiments is the potential variability in levels of silencing of a target gene, which could in turn underlie the observed phenotypic variability in the present study. Embryos with complete suppression of Hmgpi may exhibit developmental arrest at earlier stages (e.g. at the morula stage), while those with less suppression may not display a phenotype until the later stages (e.g. at the implantation stage). Ideally, the suppression level of each embryo could be experimentally analyzed to correlate with the phenotype. The third possibility is spatial translocation of HMGPI protein in the blastocyst cells. The HMGPI expression pattern indicated differential spatial requirements during early embryogenesis, supported by the apparent ability of HMGPI to shuttle between the nucleus and the cytoplasm; the cytoplasmic HMGPI observed from the 4-cell to morula stages and the nuclear HMGPI in blastocysts and ES cells could have different functions. A bipartite nuclear localization signal (NLS) peptide (FKKEKEDFQKKMRQFKK) similar to NLS of HMGN2/HMG-17 (33) is also present in the HMGPI sequence. Thus, the nuclear HMGPI in blastocysts and ES cells might exert a critical transcriptional role to regulate gene expression essential for peri-implantation development. Indeed, the siHmgpi-induced knockdown of *Hmgpi* expression downregulated *Cdx2* in trophectodermal cells and *Oct4* and *Nanog* in ICM cells, with subsequently reduced proliferation of trophectodermal cells and ICM-derived cells during blastocyst outgrowth.

Genes indispensable for derivation of ES cells

Like *Hmgpi*, *Zscan4* is another exclusively zygotic gene not expressed at any other developmental stage (13). *Zscan4* is a putative transcription factor harboring a SCAN domain and zinc finger domains, and transcribed not only in preimplantation embryos but also in ES cells (13). Reduction of *Zscan4* by RNA interference showed a phenotype similar to that induced by *Hmgpi* knockdown: developmental deterioration at the preimplantation stages, especially cleavage pause at 2-cell stage, and failure in blastocyst outgrowth, ES-cell derivation and implantation. Thus, a preimplantation-specific gene expression pattern could indicate a function in ES-cell derivation and/or maintenance. Indeed, *Hmgpi* was also expressed in entire ES colonies, whereas *Zscan4* shows a peculiar mosaic expression pattern in undifferentiated ES cell colonies. Furthermore, the *Hmgpi* gene is highly expressed in ES cells, but not in EC cells; *Hmgpi* is thus eligible as a putative ECAT (ES cell-associated transcript), whose ESTs are overrepresented in cDNA libraries from ES cells compared with those from somatic tissues and other cell lines including EC cells (34). It is also likely that *Hmgpi* is expressed in iPS cells, based on *in silico* analyses of expression profiles [NCBI GEO database, e.g. GSE10806 (35)]. Thus, *Hmgpi* is likely to have a role in maintaining pluripotent cells, since the ECATs such as *Nanog*, *Eras* and *Gdf3* are required for pluripotency and proliferation of ES cells (34,36,37). In the current study, *Hmgpi* was indeed involved in blastocyst outgrowth of ICM cells. On the other hand, several genes including ECAT members have been implicated in trophectodermal development as well as in early embryonic development. Like *Hmgpi* that was expressed in both ICM cells and trophectodermal cells, *Dnmt3l/Ecat7* has a role in embryonic and extra-embryonic tissues in early developmental stages. *DNMT3L* is recruited by *DNMT3A2* to chromatin (38) to function in DNA methylation in ES cells, and defects in maternal *DNMT3L* induce a differentiation defect in the extra-embryonic tissue (39). The reduced CDX2 expression in blastocysts and poor BrdU incorporation during blastocyst outgrowth following siHmgpi knockdown suggested the potential involvement of *Hmgpi* in trophectodermal development.

In summary, *Hmgpi* is required early on in mammalian development to generate healthy blastocysts that implant successfully and produce ES cells. HMGPI translocates into the nucleus from cytoplasm at the blastocyst stage, which is importantly a turning point of early embryonic development when DNA-methylation levels are at their lowest and implantation takes place. The nuclear HMGPI in blastocysts and ES cells is expected to act as a transcription factor to regulate gene expression networks underlying the generation, self-renewal and maintenance of pluripotent cells. Because E7 embryos have already stopped expressing *Hmgpi*, it is likely

that *Hmgpi* stage-specifically regulates a set of genes that drive peri-implantation development. It will be valuable to identify both cofactors that bind HMGPI and recognize specific DNA sequences, as well as genes that are regulated by *Hmgpi* using ES cells. A better understanding of the *Hmgpi* transcriptional network will also improve culture methods for healthy blastocysts and for generating, maintaining and differentiating ES cells.

MATERIALS AND METHODS

Identification of the mouse *Hmgpi* gene by *in silico* analysis

Preimplantation-specific genes were identified based on global gene expression profiling of oocytes and preimplantation embryos (3,40) and expressed sequence tag (EST) frequencies in the Unigene database. SMART (19) was used for domain prediction analysis. Orthologous relationships between HMG family genes were identified from phylogenetic-tree amino acid sequences determined by a sequence distance method and the Neighbor Joining (NJ) algorithm (41) using Vector NTI software (Invitrogen, Carlsbad, CA, USA).

Collection and manipulation of embryos

Six- to 8-week-old B6D2F1 mice were superovulated by injecting 5 IU of pregnant-mare serum gonadotropin (PMS; Calbiochem, La Jolla, CA, USA) followed by 5 IU of human chorionic gonadotropin (HCG; Calbiochem) 48 h later. The Institutional Review Board of the National Research Institute for Child Health and Development, Japan granted ethics approval for embryo collection from the mice. Unfertilized eggs were harvested 18 h after the HCG injection by a standard published method (42), and the cumulus cells were removed by incubation in M2 medium (EmbryoMax M-2 Powdered Mouse Embryo Culture Medium; Millipore, Billerica, MA, USA) supplemented with 300 μg/ml hyaluronidase (Sigma-Aldrich, St Louis, MO, USA). The eggs were then thoroughly washed, selected for good morphology and collected. Fertilized eggs were also harvested from mated superovulated mice in the same way as unfertilized eggs and embryos with two pronuclei (PN) were collected to synchronize *in vitro* embryo development. Fertilized eggs were cultured in synthetic oviductal medium enriched with potassium (EmbryoMax KSOM Powdered Mouse Embryo Culture Medium; Millipore) at 37°C in an atmosphere of 95% air/5% CO_2. Cultured blastocysts were transferred into pseudopregnant recipients as described previously (42). We transferred 3.5 dpc blastocysts into the uteri of 2.5 dpc pseudopregnant ICR female mice. RNA interference experiments were carried out by microinjecting <10 pl (25 ng/μl) of oligonucleotides (siHmgpi and siControl) into the cytoplasm of zygotes. The optimal siRNAs were determined by testing different concentrations (5, 10, 25 and 50 ng/μl) of three siRNAs (PE Applied Biosystems, Foster City, CA, USA), resuspended and diluted with the microinjection buffer (Millipore). Their target sequences are listed in Supplementary Material, Table S3. More than 10 independent experiments were performed to study the effect of *Hmgpi* knockdown on preimplantation development and implantation.

Culture of ES cells and blastocyst outgrowth

A mouse ES cell line (B6/129ter/sv line) was first cultured for two passages on gelatin-coated culture dishes in the presence of leukemia inhibitory factor (LIF) to remove contaminating feeder cells. Cells were then seeded on gelatin-coated 6-well plates at a density of $1-2 \times 10^5$/well ($1-2 \times 10^4$/cm^2) and cultured for 3 days in complete ES medium: KnockOut DMEM (Invitrogen) containing 15% KnockOut Serum Replacement (KSR; Invitrogen), 2000 U/ml ESGRO (mLIF; Chemicon, Temecula, CA, USA), 0.1 mM non-essential amino acids, 2 mM GlutaMax (Invitrogen), 0.1 mM beta-mercaptoethanol (2-ME; Invitrogen) and penicillin/streptomycin (50 U/50 μg/ml; Invitrogen). Blastocyst outgrowth experiments were carried out according to a standard procedure (42). In brief, zona pellucidae of blastocysts at 3.5 dpc were removed using acidic Tyrode's solution (Sigma). The blastocysts were cultured individually in the ES medium on gelatinized chamber slides at 37°C in an atmosphere of 5% CO_2. The cultured cells were examined and photographed daily. Alkaline phosphatase activity was measured using a specific detection kit (Vector Laboratories, CA, USA) after 6 days in culture. Four independent experiments were performed.

Immunostaining of oocytes and preimplantation embryos

Samples were fixed in 4% paraformaldehyde (Wako Pure Chemical, Osaka, Japan) with 0.1% glutaraldehyde (Wako) in phosphate-buffered saline (PBS) for 10 min at room temperature (RT), and then permeabilized with 0.5% Triton X-100 (Sigma) in PBS for 30 min. Immunocytochemical staining was performed by incubating the fixed samples with primary antibodies for 60 min, followed by secondary antibodies for 60 min. A polyclonal antibody to mouse HMGPI was raised in rabbits against three synthesized peptides designed according to sequence specificity, homology between mouse and human HMGPI, antigenicity, hydrophilicity and synthetic suitability [(i) CIQGHHDGAQSSRQDFTD, (ii) CMSMSGG RSSKFGRTEQS, (iii) ESPRTVSSDMKFQGC; Medical & Biological Laboratories Co, Nagoya, Japan). The anti-HMPGI was used at 1:300 dilution, followed by Alexa Fluor 546 goat anti-rabbit IgG (Molecular Probes, Invitrogen) as the secondary antibody. The anti-Histone H2B antibody (Medical & Biological Laboratories Co, Nagoya, Japan) was used at 1:300 dilution as positive control of nuclear staining, followed by Alexa Fluor 488 goat anti-mouse IgG (Molecular Probes, Invitrogen) as the secondary antibody. Blastocysts were immunostained using a monoclonal anti-Oct4 antibody (mouse IgG2b isotype, 200 μg/ml; Santa Cruz Biotechnology, Santa Cruz, CA, USA), rabbit polyclonal anti-Nanog antibody (ReproCELL, Tokyo, Japan), mouse monoclonal anti-Cdx2 antibody (CELL MARQUE, Rocklin, CA, USA), mouse monoclonal anti-BrdU antibody (Santa Cruz) and rabbit monoclonal anti-active caspase 3 (Abcam) antibody, all diluted at 1:50–300. The appropriate secondary antibodies (IgG) were diluted at 1:300 and supplied by Molecular Probes/Invitrogen: goat anti-rabbit IgG conjugated with Alexa Fluor 546 and goat anti-mouse IgG(H + L) conjugated with Alexa Fluor 488. The cellular DNA (nuclei) was stained with 4′,6-diamidino-2-phenylindole (DAPI; Wako; diluted

1:300). The cells were then washed with PBS and viewed by laser confocal microscopy (LSM510, Zeiss). For HMGPI immunostaining, all samples were processed simultaneously. The laser power was adjusted so that the signal intensity was below saturation for the developmental stage that displayed the highest intensity and all subsequent images were scanned at that laser power. This allowed us to compare signal intensities for HMGPI expression at different developmental stages. The other molecules in blastocysts and outgrowth were viewed and imaged as for the HMGPI expression.

Immunocytochemistry of blastocyst outgrowths and ES cells

Cultured ES cells and blastocyst outgrowths were fixed with 4% paraformaldehyde for 10 min at 4°C, treated with 0.1% Triton X-100 (Sigma) in PBS for 15 min at RT, and then incubated for 30 min at RT in protein-blocking solution consisting of PBS supplemented with 5% normal goat serum (Dako, Glostrup, Denmark). The samples were then incubated overnight with the primary antibodies to OCT4, HMGPI, BrdU or active caspase 3 in PBS at 4°C. The cells were then extensively washed in PBS and incubated at RT with Alexa Fluor 488 goat anti-mouse IgG1 (anti-OCT4 and anti-BrdU antibodies, diluted 1:300; Molecular Probes) or Alexa Fluor 546 goat anti-rabbit IgG(H + L) (anti-HMGPI and anti-caspase 3 antibodies, diluted 1:300), and nuclei were counterstained with DAPI for 30 min. To prevent fading, cells were then mounted in Dako fluorescent mounting medium (Dako).

Incorporation of bromodeoxyuridine (BrdU)

E3.5 blastocysts and blastocyst outgrowths were cultured for 16 h in KSOM and ES medium, respectively, supplemented with 10 μM BrdU (Sigma). Samples were then fixed in 4% paraformaldehyde for 20 min, washed in PBS and then treated with 0.5 M HCl for 30 min.

RNA extraction and real-time quantitative reverse transcriptase (qRT)–PCR

Embryos for qRT–PCR analysis were collected at 18 h post-hCG and cultured as described above. They were harvested at 0.5, 1.25, 1.75, 2.25, 2.75 and 3.75 dpc to obtain fertilized eggs 2-cell, 4-cell, 8-cell, morula and blastocyst embryos, respectively. Three subsets of 10 and 50 synchronized and intact embryos were transferred in PBS supplemented with 3 mg/ml polyvinylpyrrolidone (PVP) and stored in liquid nitrogen. Total RNA from 10 and 50 embryos was extracted using the PicoPure RNA Isolation Kit (Arcturus, La Jolla, CA, USA). The reverse transcription reaction, primed with polyA primer, was performed using Superscript III reverse transcriptase (Invitrogen) following the manufacturer's instructions. Total RNA isolated was reverse transcribed in a 20 μl volume. The resulting cDNA was quantified by qRT–PCR analysis using the SYBR Green Realtime PCR Master Mix (Toyobo, Osaka, Japan) and ABI Prism 7700 Sequence Detection System (PE Applied Biosystems) as described previously (43). An amount of cDNA equivalent to 1/2 an embryo was used for each real-time PCR reaction with a minimum of three replicates, with no-RT and no-template controls for each gene. Data were normalized against *H2afz* by the ΔΔCt method (44). PCR primers for the genes of *Hmgpi, H2afz* and *Gapdh* were listed in Supplementary Material, Table S4. Calculations were automatically performed by ABI software (Applied BioSystems). For alpha-amanitin studies, fertilized eggs were first harvested at 18 h post-hCG, instead of eggs already advanced to the two-pronucleus stage. After 3 h of incubation, eggs that carried both male and female pronuclei were selected at 21 h post-hCG and randomly assigned to two experimental groups: with and without addition of alpha-amanitin to the culture medium. The eggs were further cultured in KSOM at 37°C in an atmosphere of 5% CO_2 until the specified time point (32, 43 and 54 h post-hCG). Embryos used for alpha-amanitin studies and RNA interference experiments were subjected to qRT–PCR as described for the normal preimplantation embryos.

Immunoblot analysis

Protein samples from embryos were solubilized in Sample Buffer Solution without 2-ME (Nacalai Tesque, Kyoto, Japan), resolved by NuPAGE Novex on Tris-acetate mini gels (Invitrogen), and transferred to Immobilon-P transfer membrane (Millipore). The membrane was soaked in protein blocking solution (Blocking One solution, Nacalai) for 30 min at RT before an overnight incubation at 4°C with primary antibody, also diluted in blocking solution. The membrane was then washed three times with TBST (Tris-buffered saline with 0.1% Tween-20), incubated with a horseradish peroxidase-conjugated secondary antibody (0.04 μg/ml) directed against the primary antibody for 60 min, and washed three times with TBST. The signal was detected by enhanced chemiluminescence (SuperSignal West Dura Extended Duration Substrate, Thermoscientific, Rockford, IL, USA) following the manufacturer's recommendations. The intensity of the band was quantified using NIH Image J software. Briefly, the signal was outlined and the mean intensity and background fluorescence were measured. The specific signal was calculated by dividing the band intensities for HMGPI by those for actin.

Statistical analysis

Differences between groups were evaluated statistically using Student's *t*-test or ANOVA, with P-values < 0.05 considered significant.

SUPPLEMENTARY MATERIAL

Supplementary Material is available at *HMG* online.

ACKNOWLEDGEMENTS

The authors would like to thank Dr Takashi Hiiragi for valuable advice and critical reading of the manuscript.

Conflict of Interest statement. The authors declare that there is no conflict of interest that would prejudice the impartiality of the scientific work.

FUNDING

This work was supported, in part, by Grants-in-Aid from the Japan Society for the Promotion of Science (19591911 to T.H., 21390456 to H.A.), by a National Grant-in-Aid from Japanese Ministry of Health, Labor, and Welfare (H21-001, H20-001 to T.H., H18-004 to H.A. and N.K.) and by a Grant-in-Aid from the Yamaguchi- Endocrine Organization to T.H. Funding to pay the Open Access publication charges for this article was provided by Grants-in-Aid for Young Scientists (B) (21791581 to M.Y.).

REFERENCES

1. DePamphilis, M.L., Kaneko, K.J. and Vassilev, A. (2002) Activation of zygotic gene expression in mammals. DePamphilis, M.L. (ed.), *Advances in Developmental Biology and Biochemistry*, Vol. 12, Elsevier Science, B.V.
2. Latham, K.E. and Schultz, R.M. (2001) Embryonic genome activation. *Front. Biosci.*, **6**, D748–D759.
3. Hamatani, T., Carter, M.G., Sharov, A.A. and Ko, M.S. (2004) Dynamics of global gene expression changes during mouse preimplantation development. *Dev. Cell.*, **6**, 117–131.
4. Takahashi, K. and Yamanaka, S. (2006) Induction of pluripotent stem cells from mouse embryonic and adult fibroblast cultures by defined factors. *Cell*, **126**, 663–676.
5. Hamatani, T., Yamada, M., Akutsu, H., Kuji, N., Mochimaru, Y., Takano, M., Toyoda, M., Miyado, K., Umezawa, A. and Yoshimura, Y. (2008) What can we learn from gene expression profiling of mouse oocytes? *Reproduction*, **135**, 581–592.
6. Ko, M.S., Kitchen, J.R., Wang, X., Threat, T.A., Hasegawa, A., Sun, T., Grahovac, M.J., Kargul, G.J., Lim, M.K., Cui, Y. *et al.* (2000) Large-scale cDNA analysis reveals phased gene expression patterns during preimplantation mouse development. *Development*, **127**, 1737–1749.
7. Okazaki, Y., Furuno, M., Kasukawa, T., Adachi, J., Bono, H., Kondo, S., Nikaido, I., Osato, N., Saito, R., Suzuki, H. *et al.* (2002) Analysis of the mouse transcriptome based on functional annotation of 60,770 full-length cDNAs. *Nature*, **420**, 563–573.
8. Solter, D., de Vries, W.N., Evsikov, A.V., Peaston, A.E., Chen, F.H. and Knowles, B.B. (2002) Fertilization and activation of the embryonic genome. Rossant, J. and Tam, P.P.L. (eds), *Mouse Development: Patterning, Morphogenesis, and Organogenesis.*, Academic Press, San Diego, pp. 5–19.
9. Wang, Q.T., Piotrowska, K., Ciemerych, M.A., Milenkovic, L., Scott, M.P., Davis, R.W. and Zernicka-Goetz, M. (2004) A genome-wide study of gene activity reveals developmental signaling pathways in the preimplantation mouse embryo. *Dev. Cell.*, **6**, 133–144.
10. Wang, S., Cowan, C.A., Chipperfield, H. and Powers, R.D. (2005) Gene expression in the preimplantation embryo: in-vitro developmental changes. *Reprod. Biomed. Online*, **10**, 607–616.
11. Zeng, F., Baldwin, D.A. and Schultz, R.M. (2004) Transcript profiling during preimplantation mouse development. *Dev. Biol.*, **272**, 483–496.
12. Choo, K.B., Chen, H.H., Cheng, W.T., Chang, H.S. and Wang, M. (2001) In silico mining of EST databases for novel pre-implantation embryo-specific zinc finger protein genes. *Mol. Reprod. Dev.*, **59**, 249–255.
13. Falco, G., Lee, S.L., Stanghellini, I., Bassey, U.C., Hamatani, T. and Ko, M.S. (2007) Zscan4: a novel gene expressed exclusively in late 2-cell embryos and embryonic stem cells. *Dev. Biol.*, **307**, 539–550.
14. Kanka, J. (2003) Gene expression and chromatin structure in the pre-implantation embryo. *Theriogenology*, **59**, 3–19.
15. Schultz, R.M. and Worrad, D.M. (1995) Role of chromatin structure in zygotic gene activation in the mammalian embryo. *Semin. Cell Biol.*, **6**, 201–208.
16. Thompson, E.M., Legouy, E. and Renard, J.P. (1998) Mouse embryos do not wait for the MBT: chromatin and RNA polymerase remodeling in genome activation at the onset of development. *Dev. Genet.*, **22**, 31–42.
17. Stros, M., Launholt, D. and Grasser, K.D. (2007) The HMG-box: a versatile protein domain occurring in a wide variety of DNA-binding proteins. *Cell. Mol. Life Sci.*, **64**, 2590–2606.
18. Zhang, Q. and Wang, Y. (2008) High mobility group proteins and their post-translational modifications. *Biochim. Biophys. Acta*, **1784**, 1159–1166.
19. Schultz, J., Milpetz, F., Bork, P. and Ponting, C.P. (1998) SMART, a simple modular architecture research tool: identification of signaling domains. *Proc. Natl Acad. Sci. USA*, **95**, 5857–5864.
20. Mamo, S., Gal, A.B., Bodo, S. and Dinnyes, A. (2007) Quantitative evaluation and selection of reference genes in mouse oocytes and embryos cultured in vivo and in vitro. *BMC Dev. Biol.*, **7**, 14.
21. Hock, R., Furusawa, T., Ueda, T. and Bustin, M. (2007) HMG chromosomal proteins in development and disease. *Trends Cell Biol.*, **17**, 72–79.
22. Svarcova, O., Dinnyes, A., Polgar, Z., Bodo, S., Adorjan, M., Meng, Q. and Maddox-Hyttel, P. (2009) Nucleolar re-activation is delayed in mouse embryos cloned from two different cell lines. *Mol. Reprod. Dev.*, **76**, 132–141.
23. Sanij, E., Poortinga, G., Sharkey, K., Hung, S., Holloway, T.P., Quin, J., Robb, E., Wong, L.H., Thomas, W.G., Stefanovsky, V. *et al.* (2008) UBF levels determine the number of active ribosomal RNA genes in mammals. *J. Cell Biol.*, **183**, 1259–1274.
24. Stefanovsky, V.Y., Pelletier, G., Hannan, R., Gagnon-Kugler, T., Rothblum, L.I., Moss, T., Bazett-Jones, D.P. and Crane-Robinson, C. (2001) An immediate response of ribosomal transcription to growth factor stimulation in mammals is mediated by ERK phosphorylation of UBF DNA looping in the RNA polymerase I enhancesome is the result of non-cooperative in-phase bending by two UBF molecules. *Mol. Cell.*, **8**, 1063–1073.
25. Stefanovsky, V.Y., Pelletier, G., Bazett-Jones, D.P., Crane-Robinson, C. and Moss, T. (2001) DNA looping in the RNA polymerase I enhancesome is the result of non-cooperative in-phase bending by two UBF molecules. *Nucleic Acids Res.*, **29**, 3241–3247.
26. Mais, C., Wright, J.E., Prieto, J.L., Raggett, S.L. and McStay, B. (2005) UBF-binding site arrays form pseudo-NORs and sequester the RNA polymerase I transcription machinery. *Genes Dev.*, **19**, 50–64.
27. Falciola, L., Spada, F., Calogero, S., Langst, G., Voit, R., Grummt, I. and Bianchi, M.E. (1997) High mobility group 1 protein is not stably associated with the chromosomes of somatic cells. *J. Cell Biol.*, **137**, 19–26.
28. Bonaldi, T., Talamo, F., Scaffidi, P., Ferrera, D., Porto, A., Bachi, A., Rubartelli, A., Agresti, A. and Bianchi, M.E. (2003) Monocytic cells hyperacetylate chromatin protein HMGB1 to redirect it towards secretion. *EMBO J.*, **22**, 5551–5560.
29. Wang, H., Bloom, O., Zhang, M., Vishnubhakat, J.M., Ombrellino, M., Che, J., Frazier, A., Yang, H., Ivanova, S., Borovikova, L. *et al.* (1999) HMG-1 as a late mediator of endotoxin lethality in mice. *Science*, **285**, 248–251.
30. Cui, X.S., Shen, X.H. and Kim, N.H. (2008) High mobility group box 1 (HMGB1) is implicated in preimplantation embryo development in the mouse. *Mol. Reprod. Dev.*, **75**, 1290–1299.
31. Payer, B., Saitou, M., Barton, S.C., Thresher, R., Dixon, J.P., Zahn, D., Colledge, W.H., Carlton, M.B., Nakano, T. and Surani, M.A. (2003) Stella is a maternal effect gene required for normal early development in mice. *Curr. Biol.*, **13**, 2110–2117.
32. Gurtu, V.E., Verma, S., Grossmann, A.H., Liskay, R.M., Skarnes, W.C. and Baker, S.M. (2002) Maternal effect for DNA mismatch repair in the mouse. *Genetics*, **160**, 271–277.
33. Hock, R., Scheer, U. and Bustin, M. (1998) Chromosomal proteins HMG-14 and HMG-17 are released from mitotic chromosomes and imported into the nucleus by active transport. *J. Cell Biol.*, **143**, 1427–1436.
34. Mitsui, K., Tokuzawa, Y., Itoh, H., Segawa, K., Murakami, M., Takahashi, K., Maruyama, M., Maeda, M. and Yamanaka, S. (2003) The homeoprotein Nanog is required for maintenance of pluripotency in mouse epiblast and ES cells. *Cell*, **113**, 631–642.
35. Kim, J.B., Zaehres, H., Wu, G., Gentile, L., Ko, K., Sebastiano, V., Arauzo-Bravo, M.J., Ruau, D., Han, D.W., Zenke, M. *et al.* (2008)